AMERICAN SOCIETY FOR MICROBIOLOGY | Journal of Virology

Generation of Long-Lived Bone Marrow Plasma Cells Secreting Antibodies Specific for the HIV-1 gp41 Membrane-Proximal External Region in the Absence of Polyreactivity

Luke R. Donius,[a] Yuxing Cheng,[a*] Jaewon Choi,[a*] Zhen-Yu J. Sun,[b] Melissa Hanson,[c*] Michael Zhang,[c*] Todd M. Gierahn,[f] Susanna Marquez,[d] Mohammed Uduman,[d] Steven H. Kleinstein,[d,e] Darrell Irvine,[c,f,g] J. Christopher Love,[f] Ellis L. Reinherz,[a] Mikyung Kim[a,h]

Laboratory of Immunobiology and Department of Medical Oncology, Dana-Farber Cancer Institute, Boston, Massachusetts, USA[a]; Department of Biological Chemistry & Molecular Pharmacology, Harvard Medical School, Boston, Massachusetts, USA[b]; Departments of Materials Science and Engineering and Biological Engineering, Massachusetts Institute of Technology, Cambridge, Massachusetts, USA[c]; Department of Pathology, Yale School of Medicine, New Haven, Connecticut, USA[d]; Department of Immunology, Yale School of Medicine, and Interdepartmental Program in Computational Biology and Bioinformatics, Yale University, New Haven, Connecticut, USA[e]; Koch Institute for Integrative Cancer Research at MIT, Cambridge, Massachusetts, USA[f]; Howard Hughes Medical Institute, Chevy Chase, Maryland, USA[g]; Department of Dermatology, Harvard Medical School, Boston, Massachusetts, USA[h]

ABSTRACT

An effective preventive vaccine is highly sought after in order to stem the current HIV-1 pandemic. Both conservation of contiguous gp41 membrane-proximal external region (MPER) amino acid sequences across HIV-1 clades and the ability of anti-MPER broadly neutralizing antibodies (BNAbs) to block viral hemifusion/fusion establish the MPER as a prime vaccination target. In earlier studies, we described the development of an MPER vaccine formulation that takes advantage of liposomes to array the MPER on a lipid bilayer surface, paralleling its native configuration on the virus membrane while also incorporating molecular adjuvant and CD4 T cell epitope cargo. Here we demonstrate that several immunizations with MPER/liposomes induce high levels of bone marrow long-lived plasma cell (LLPC) antibody production. Single-cell immunoglobulin gene retrieval analysis shows that these plasma cells are derived from a germ line repertoire of B cells with a diverse representation of immunoglobulin genes, exhibiting antigen-driven positive selection. Characterization of LLPC recombinant monoclonal antibodies (rMAbs) indicates that antigen recognition is achieved through convergence on a common epitopic focus by utilizing various complementarity-determining region H3 (CDRH3) lengths. Importantly, the vast majority of rMAbs produced from these cells lack polyreactivity yet manifest antigen specificity in the context of lipids, shaping MPER-specific paratopes through selective pressure. Taken together, these findings demonstrate that the MPER is a vaccine target with minimal risk of generating off-target autoimmunity.

IMPORTANCE

A useful vaccine must generate desired long-term, antigen-specific antibody responses devoid of polyreactivity or autoreactivity. The common polyreactive features of some HIV-1 BNAbs have raised concern about elicitation of anti-MPER antibodies. Utilizing single-LLPC repertoire analysis and biophysical characterization of anti-MPER rMAbs, we show that their fine specificities require a structural fitness of the antibody combining site involving heavy and light chain variable domains shaped by somatic hypermutation and affinity maturation of B cells in the germinal center. Perhaps more importantly, our results demonstrate that the majority of MPER-specific antibodies are not inherently polyspecific and/or autoreactive, suggesting that polyreactivity of MPER-specific antibodies is separable from their antigen specificity.

To date, no widely applicable cure for HIV-1 is known, and current preventive efforts have not proven completely effective. Successful vaccination would be a powerful means to fight the global HIV-1 pandemic. Unlike infectious diseases against which vaccines induce highly protective immunity (1), broad and potent neutralization of HIV-1 strains has not been elicited through vaccination with HIV-1 protein envelope (Env) subunits or inactivated virus. However, the discovery of numerous broadly neutralizing antibodies (BNAbs) capable of blocking viral binding to or entry into host cells suggested that vaccination is a promising strategy (2–4).

The HIV-1 envelope spike protein, comprised of trimeric gp41 and gp120 subunits, is the only viral target exposed on the virion membrane surface and therefore is the singular focus for an antibody-based vaccine. The first HIV-1 BNAb discovered, 2F5, is specific for the membrane-proximal external region (MPER), and more recently, the MPER-specific neutralizing antibody list has grown to include 4E10, Z13e1, m66, m66.6, 10E8, and CAP206-

Received 3 June 2016 **Accepted** 18 July 2016

Accepted manuscript posted online 27 July 2016

Citation Donius LR, Cheng Y, Choi J, Sun Z-YJ, Hanson M, Zhang M, Gierahn TM, Marquez S, Uduman M, Kleinstein SH, Irvine D, Love JC, Reinherz EL, Kim M. 2016. Generation of long-lived bone marrow plasma cells secreting antibodies specific for the HIV-1 gp41 membrane-proximal external region in the absence of polyreactivity. J Virol 90:8875–8890. doi:10.1128/JVI.01089-16.

Editor: F. Kirchhoff, Ulm University Medical Center

Address correspondence to Mikyung Kim, mikyung_kim@dfci.harvard.edu.

* Present address: Yuxing Cheng, Pfizer, Cambridge, Massachusetts, USA; Jaewon Choi, Bristol Myers Squibb, Devens, Massachusetts, USA; Melissa Hanson, Institut Pasteur, Paris, France; Michael Zhang, University of Maryland, Baltimore, Maryland, USA.

L.R.D. and Y.C. contributed equally to this article.

CH12 (5–12). The BNAb list has also widened over time with the identification of a variety of other targets, including the CD4-binding site, the V1/V2-glycan-containing epitope, the V3-glycan-containing epitope, and gp120/gp41-bridging epitopes. These BNAbs were discovered through the recovery of single memory B cells from infected individuals and by recombinant monoclonal antibody (rMAb) production (reviewed in references 2, 13, and 14). Nevertheless, as one of the most highly conserved regions on the envelope spike, the MPER remains an exemplary vaccine target (9, 15, 16).

The MPER is a hydrophobic and tryptophan-rich segment of 22 amino acids located immediately external to the transmembrane (TM) domain of gp41 (15, 17). Structurally, the MPER consists of two alpha-helices connected by a linker in a helix-hinge-helix motif in a lipid environment (16, 18). We previously showed that the BNAbs 2F5 and 4E10 mediate extraction of their epitopic residues on the MPER helices from the lipid membrane (18–20). Very recently, the first micelle-embedded trimer spike structure that includes the MPER and TM regions was elegantly solved using cryo-electron microscopy (cryo-EM), and this structure suggests that in a 10E8-bound conformation, the MPER is lifted up off the membrane (21). A recent crystallographic analysis identified a lipid as an integral component of the 4E10 BNAb and implied a similar MPER segment extraction geometry out of the membrane (22). Functionally, the MPER has been shown to be required for both hemifusion and fusion processes preceding viral entry (15–17, 23–25), presumably through its strong interaction with the membrane. Therefore, antibodies elicited by vaccination that bind with high affinity to the MPER on the trimer would impede or block MPER function and manifest neutralizing activity.

Extensive biochemical and structural analyses of MPER-specific BNAbs have suggested the obligate role of the membrane environment in MPER immunogen design, both to configure native MPER structure and to induce potent BNAbs (18, 19, 22, 26–35). Such requirements are likely explanations for the lack of anti-MPER neutralizing antibodies elicited through vaccination with free MPER peptides, MPER epitope mimetics, or MPER epitopes grafted onto protein scaffolds (28, 36–38; reviewed in reference 39). Nonetheless, while liposome-based MPER vaccines induce strong MPER antibody responses (40–45), the chemical modifications used for membrane anchoring and prevention of proteolysis, such as palmitic acid adducts and amide capping, respectively, have an impact on antigenic determinants even without inducing alterations in the MPER segment structure (42). These challenges for membrane-arrayed MPER segment immunogen design still await innovative solutions. Moreover, it has been proposed that sequence similarity of endogenous mammalian proteins to the MPER limits expansion of B cells expressing germ line-encoded MPER-reactive B cell receptors (BCR) because of negative selection during development (46, 47). It has further been suggested that HIV-1 Env gp41 antibodies might arise from polyreactive B cells, possibly from the pool of gut microbe-regulating B cells (48, 49). This notion might explain why acutely HIV-1-infected subjects have antibodies whose unmutated ancestors react with bacterial or host antigens but not with the HIV-1 envelope. The highly polyreactive nature of the MPER BNAbs 2F5 and 4E10 has been construed as evidence for the existence of such a pathway (47, 50, 51). These are sound proposals; however, given the ability of certain BNAbs, notably 10E8, to arise independently of polyreactivity (6), it is not a *sine qua non* that a successful MPER immunogen must elicit antibodies with this characteristic in order to be broadly neutralizing.

In this study, we experimentally assessed the extent to which durable, affinity-matured anti-MPER antibody responses induced by MPER/liposome vaccination exhibit polyreactivity. We demonstrated that MPER/liposome immunizations generate MPER-specific bone marrow (BM) long-lived plasma cell (LLPC)-derived class-switched Abs. Single-plasma-cell analysis followed by immunoglobulin gene rescue and sequencing and analysis of expressed rMAbs revealed that BM LLPC use a diverse collection of immunoglobulin genes with the same epitope specificity, but with functionally distinct characteristics. Affinity maturation of multiple distinct B cells postimmunization and -boosting yielded MPER epitope specificity through structural fitness and convergence on a common antigenic determinant, accompanied by little, if any, polyreactivity for 39 of 44 rMAbs analyzed. These characteristics demonstrate that MPER specificity is not defined by polyreactivity for the vast majority of rMAbs elicited by vaccination that recognize membrane-embedded MPER.

MATERIALS AND METHODS

Mice and MPER/liposome immunizations. BALB/c mice were obtained from Taconic Biosciences (Hudson, NY). All mice used were 8 to 10 weeks of age at the time of initial immunization. Mice were housed in a specific-pathogen-free facility and maintained in accordance with procedures and protocols approved by the Dana-Farber Cancer Institute and Harvard Medical School Animal Care and Use Committee Institutional Review Board. Immunization liposomes were made as described before (42) by drying the following components under a nitrogen stream and placing them under vacuum overnight: N- or C-terminally palmitoylated MPER peptides (Npalm-MPER or Cpalm-MPER), monophosphoryl lipid A (MPLA) from *Salmonella enterica* serotype Minnesota (Sigma-Aldrich, St. Louis, MO), and the lipids 1,2-dioleoyl-*sn*-glycero-3-phosphocholine (DOPC), 1,2-dimyristoyl-*sn*-glycero-3-phosphocholine (DMPC), and 1,2-dioleoyl-*sn*-glycero-3-phospho-(1′-*rac*-glycerol) (DOPG) (Avanti Polar Lipids Inc., Alabaster, AL) at a 2:2:1 ratio. Liposomes were formed with encapsulated LACK1 peptide by rehydration with phosphate-buffered saline (PBS) containing 1,000 μg/ml LACK1 to a final total liposome component of 25.2 mg/ml. Final liposomes incorporated MPER at a 1:200 molar ratio (MPER:lipid) and contained 175 μg/ml MPLA, with a total lipid concentration of 25 mg/ml. MPER/liposomes were sized by vortexing 6 times for 30 s each at 5-min intervals, 6 rounds of flash freezing in liquid nitrogen and thawing at 37°C, and extrusion by passage through a 100-nm-pore-size polycarbonate membrane 21 times. Mice were immunized intradermally with 50 μl per hind flank. Unless noted otherwise, immunizations were administered on three occasions at 21-day intervals.

Microengraving and single-B-cell isolation. Npalm-MPER/liposomes, consisting of MPER at a 1:50 molar ratio with DOPC and DOPG lipids (4:1) at a final total liposome component of 2 mg/ml, were rehydrated by vortexing, freeze-thawing, and extrusion as described above. Polylysine-coated glass slides (25 × 75 × 1 mm) were incubated overnight with rocking at room temperature, submerged in 100 μg/ml liposomes in PBS. The liposome solution was poured off, and slides were blocked for 1 h in a 3% milk-0.05% Tween 20-PBS solution with rocking at room temperature. Polymethylsiloxane microwell molds were prepared as described in detail by Ogunniyi et al. (52). Molds were subjected to plasma cleaning under vacuum to charge and sterilize the surface and then were blocked with 1% bovine serum albumin (BSA) in PBS for 20 min. The blocking solution was rinsed from slides with purified water. $CD138^+$ plasma cells were sorted from the BM of femurs and tibias from one mouse by use of a Miltenyi Biotec (Bergisch Gladbach, Germany) magnetic bead labeling and enrichment kit. The mold was removed from blocking buffer and the liquid aspirated, followed by three washes with

10% fetal bovine serum containing 1% penicillin-streptomycin in RPMI 1640 (growth medium). The growth medium was aspirated, and plasma cells (~100,000 in 300 μl growth medium) were distributed dropwise evenly across the mold. The growth medium in the mold was aspirated, and growth medium was distributed onto the mold surface. The medium was then aspirated, and growth medium plus 100 ng/ml interleukin-6 (IL-6) was distributed on the mold before the MPER/liposome-labeled slide was placed on the mold and clamped in place in a hybridization chamber for 1 h at 37°C. Following incubation, the slide was washed and blocked, and secondary antibody (goat anti-mouse IgG–AF647 and anti-IL-6–AF488) hybridization was carried out in a Tecan HS 400 Pro slide washer (Tecan, Mannedorf, Switzerland). Microarray analysis of slides was performed using a GenePix 4400 instrument (Molecular Devices LLC, Sunnyvale, CA) at 488 nm and 635 nm, and identification of wells containing MPER-specific cells was performed using GenePix Pro 6 analysis software. The mold with plasma cells was stored submerged in growth medium at 4°C overnight, and single plasma cells were isolated by use of a micromanipulator and placed into 96-well plates containing a solution of 1 μl RNasin Plus RNase inhibitor (Promega, Madison, WI) and 9 μl UltraPure DNase-/RNase-free H_2O (Life Technologies, Grand Island, NY). Plates were sealed and stored at −80°C for later RNA isolation/cDNA synthesis.

MPER-specific single-B-cell cDNA generation, PCR, and cloning. Our method for cloning and expression of mouse immunoglobulin genes from single B cells was adopted from the method developed by Tiller et al. (53) and utilized the primers and vectors they described. In brief, 96-well plates with single B cells were thawed on ice, and 5 μl of reverse transcription primer mix (1 μl random primers, 1 μl deoxynucleoside triphosphates [dNTPs] [10 mM concentration of each], 1 pmol [each] 1st-round PCR reverse heavy and kappa light chain [IgH and IgLk] primers, and DNase/RNase-free water) was added to each well. The plate was heated to 65°C for 5 min in a thermocycler and then cooled on ice for 1 min. SuperScript3 reverse transcription mix containing 5× reverse transcription buffer, dithiothreitol (DTT), RNase Out, SuperScript3, and DNase/RNase-free water was added to a final volume of 30 μl, and cDNA synthesis was performed by running the following ramped thermocycler program: 25°C for 5 min, 50°C for 60 min, 55°C for 60 min, and 70°C for 15 min. A nested PCR strategy was used to amplify the IgH or IgLk immunoglobulin gene from cDNA. First- and second-round nested PCRs were performed using high-fidelity Q5 polymerase (New England BioLabs, Ipswich, MA). For IgH amplification, 3 μl of cDNA reaction mix was added to a total of 50 μl of PCR mix and amplified using the following program: 98°C for 30 s, 50 cycles of 98°C for 30 s, 50°C for 30 s, and 72°C for 30 s, and a final extension at 72°C for 10 min. The same strategy was implemented for IgLk amplification, but with a 47°C annealing temperature instead of 50°C. The second-round PCR was performed using 1 μl of the first-round template for nested amplification with the same thermocycler programs as those described above. DNA sequences were obtained using the second-round PCR 5′ primer mix. IgH and IgLk pairs of interest were cloned by determining the closest-matching V-gene/J-gene cloning primer sets described by Tiller et al. and reamplifying the sequence from the first-round PCR product. The resulting fragment was gel purified, inserted into the pCR-BLUNT II TOPO vector by use of topoisomerase I (Zero Blunt TOPO cloning kit; Thermo Fisher, Waltham, MA), and transfected into *Escherichia coli* for subcloning (One-Shot TOP10 chemically competent cells; Thermo Fisher, Waltham, MA). Plasmids were isolated, sequenced to confirm fidelity, and restriction digested for insertion into the IgH and IgLk expression vectors for human IgG1 and kappa chain, respectively. Expression of rMAbs was performed by transfecting 30-ml cultures of exponential-growth-phase 293F cells with 20 μg each of IgH and IgLk in their respective vectors by use of 293Fectin (Thermo Fisher, Waltham, MA) with shaking in a cell culture incubator at 37°C and 5% CO_2 for 7 days. Expressed rMAbs were isolated by pelleting cells, filtering the supernatants to 0.22 μm, purifying immunoglobulin by use of Gamma-bind Plus Sepharose beads (GE Healthcare, Little Chalfont, United Kingdom), and concentrating the samples with 30K centrifugal filters.

MPER/liposome and cardiolipin/dsDNA ELISAs. Enzyme-linked immunosorbent assays (ELISAs) for measuring MPER-specific antibodies from sera were done by labeling Immulon 1B plates overnight with 2 μg/ml streptavidin in PBS (50 μl/well) at 4°C. The following day, plates were washed three times with 0.1% BSA-PBS and blocked with 100 μl per well 1% BSA-PBS for 3 h. Incubation with 0.2% biotinylated polyethylene glycol (PEG) 2000-containing Npalm-MPER-NH_2/liposomes or Npalm-MPER-COOH/liposomes (1:50 peptide:lipid ratio) at 32 μg/ml in 1% BSA-PBS was then carried out for 2 h with shaking at room temperature and then for another 2 h at 4°C. Plates were then washed again, and serially diluted sera in 1% BSA-PBS were aliquoted and incubated overnight with gentle rocking at 4°C. The following day, serum samples were removed, the plate was washed, and goat anti-mouse–horseradish peroxidase (HRP) secondary antibody (Bio-Rad, Hercules, CA) at a 1:2,000 dilution was applied for 1 h at 4°C. Plates were washed two times with 0.1% BSA-PBS and two times with PBS. Bound antibody was detected by incubation with *o*-phenylenediamine (OPD) solution in citrate buffer, pH 4.5, for 10 min. The OPD reaction was stopped with 2.25 M H_2SO_4, and the absorbance was read at 490 nm on a Victor X4 plate reader (Perkin-Elmer, Waltham, MA). Autoreactivity/polyreactivity of MPER-specific rMAbs was tested by ELISAs with cardiolipin and double-stranded DNA (dsDNA) by coating Immulon 2HB plates (Thermo Scientific, Waltham, MA) with 75 μg/ml cardiolipin (Sigma-Aldrich, St. Louis, MO) in ethanol and allowing them to air dry overnight or coating them with 100 μg/ml of sheared 0.45-μm-filtered salmon sperm DNA (Life Technologies, Grand Island, NY) in PBS overnight at 4°C. Plates were washed three times with 0.05% Tween 20-PBS, and all wells were blocked with 1% BSA-PBS for 1 h at room temperature with shaking. Plates were washed with 0.05% Tween 20-PBS, and serially diluted rMAbs were incubated for 1 h at room temperature. Washing was repeated, and the wells were incubated with 1:3,000 goat anti-human IgG–HRP (Bio-Rad, Hercules, CA) antibody for 1 h at room temperature. Plates were washed six times with 0.05% Tween 20-PBS, and bound antibody was detected using OPD solution as described above. Non-antigen-coated plates were set up in parallel to measure nonspecific binding and to subtract the background signal from the total.

ELISPOT quantification of MPER-specific ASCs. Enzyme-linked immunosorbent spot (ELISPOT) analysis for quantifying the numbers of antigen-specific antibody-secreting cells (ASCs) from BM, spleens, and lymph nodes was performed using 96-well 0.45-μm, hydrophobic, high-protein-binding Immobilon-P polyvinylidene difluoride (PVDF) membrane plates (EMD Millipore, Billerica, MA). Plates were activated with 35% ethanol and then washed eight times with water, followed by incubation with 100 μl per well of various 100-μg/ml Npalm-MPER/liposome formulations in PBS (1:50 or 1:1,000 MPER:lipid ratio; 4:1 DOPC:DOPG ratio) overnight at 4°C. Plates were washed six times with 0.1% BSA-PBS, blocked with 200 μl/well 1% BSA-PBS for at least 4 h, washed once with RPMI 1640 medium supplemented with 10% FBS, glutamine, 2-mercaptoethanol, and penicillin-streptomycin, and then blocked for 1 h at 37°C with the same medium. Meanwhile, mouse spleens, inguinal lymph nodes (iLN), and BM were isolated, and single-cell suspensions were prepared in the aforementioned growth medium. Cells were strained to 70 μm, quantified using a hemacytometer, and resuspended to 1×10^7 cells/ml. The growth medium block was removed from plates and replaced with 50 μl/well fresh growth medium. Cell suspensions were restrained to 70 μm and added to wells in 50-μl volumes (500,000 cells), in triplicate or quadruplicate. Hybridoma cells (M1) which secrete a C-terminal MPER-specific antibody and BNAb 2F5-expressing cells were plated as controls. Cells were incubated overnight at 37°C and 5% CO_2 in a humidified chamber. The following day, wells were washed six times with 0.1% BSA-PBS and blocked for 1.5 h with 1% BSA-PBS. The blocking buffer was discarded, and bound antibody was detected using 0.6 μg/ml of alkaline phosphatase (AP)-conjugated goat anti-mouse secondary antibodies

(anti-IgM, anti-IgG1, anti-IgG2a, anti-IgG2b, anti-IgG3, and anti-IgG; Jackson ImmunoResearch, West Grove, PA) in 1% BSA-PBS. BNAb 2F5-secreting control cells were visualized using goat anti-human IgG–AP. To visualize MPER-specific bound antibody, wells were washed eight times, and 100 μl/well 5-bromo-4-chloro-3-indolyl phosphate/nitro blue tetrazolium (BCIP/NBT) solution was added for 5 min. Plates were washed thoroughly with distilled water and dried overnight. Spots were quantified using a CTL ImmunoSpot ELISPOT plate reader and ImmunoSpot 3 software (CTL, Shaker Heights, OH).

SPR analysis. Surface plasmon resonance (SPR) analysis was done as described previously (42). Briefly, for alanine scanning analysis, 30 μl of 150 μM-250 μM DOPC-DOPG liposomes in running buffer (20 mM HEPES, 0.15 mM NaCl, pH 7.4) was applied to a Pioneer L1 sensor chip in a BIAcore 3000 instrument at a flow rate of 3 μl/min at 25°C. Multilamellar structures were removed by injection of 20 μl of 25 mM sodium hydroxide at a flow rate of 100 μl/min. MPER peptides (0.5 μM) were dissolved in running buffer right before injection and complexed with the liposomes by injection of 60 μl at a flow rate of 10 μl/min. Binding of MAb was then tested by passage of the MAb over the peptide-liposome complex at 10 μl/min. Peptide-liposome complexes were removed by sequential passages of 40 mM 3-[(3-cholamidopropyl)-dimethylammonio]-1-propanesulfonate (CHAPS) and 3:2 sodium hydroxide (50 mM)-isopropyl alcohol over the sensor chip. For liposome-only or MPER/liposome rMAb binding analysis, 30 μl of each purified rMAb at 30 μg/ml was applied to the chip at a flow rate of 10 μl/min for 3 min, using a protocol identical to that for alanine scanning analysis (42).

Immunoglobulin gene sequence analysis. Immunoglobulin genes from two mice ($n = 66$ total sequences generated) were amplified from single MPER-specific IgG-secreting plasma cells. The sequences were aligned by use of IMGT/HighV-QUEST (version 1.5.1) to identify their V(D)J germ line segments. Sequences for which a junction could not be identified ($n = 18$) were excluded from further analyses, leaving 15 sequences for mouse 1 and 33 for mouse 2 for detailed investigation. Downstream analyses were performed using tools from the Change-O suite (version 0.3.3-2016.04.22) and the associated R packages SHazaM (shazam_0.1.2.999) and alakazam (alakazam_0.2.3.999) (54). Detailed information is available at http://immcantation.readthedocs.io. Sequences were assigned to the same clone when they shared the same IGHV gene, IGHJ gene, IGLkV gene, IGLkJ gene, and junction length, with a Hamming distance threshold of 0.05, using the DefineClones command line tool. For each clone, the germ line sequences were identified for the heavy and light chains by use of the CreateGermlines tool, and the germ line definitions were retrieved from IMGT (as of 2 May 2016). SHazaM was used to quantify the mutation frequencies for the V segment up to the start of CDR3 by comparison to the IMGT germ line gene segment, and also broken down by region (complementarity-determining region [CDR], framework region [FWR], or entire sequence). BASELINe (version 1.3 [30 January 2014]) (55) was used to quantify selection strength in the CDR and FWR by using the Focused test statistic and the mouse trinucleotide SHM targeting model and selecting the clonal sequence option.

MPER constructs. MPER peptides were generated on an ABI 431 peptide synthesizer by using Fmoc chemistry, high-pressure liquid chromatography (HPLC) purification, and postpurification conjugation of N-terminal palmitic acid at the Massachusetts Institute of Technology, as described previously (42). Peptide amino acid sequences were as follows: MPER-NH_2, palm-ELDKWASLWNWFNITNWLWYIK-NH_2; MPER-COOH, palm-ELDKWASLWNWFNITNWLWYIK-COOH; W680A-COOH, palm-ELDKWASLWNWFNITNWLAYIK-COOH; MPER-N, palm-GSGSDLLELDKWASLWNWFNIT-NH_2; and MPER-C, palm-GGGSSASLWNWFNITNWLWYIK-NH_2.

RESULTS

MPER/liposome immunizations generate antigen-specific LLPC. Circulating high-affinity antibodies are maintained for decades by LLPC without reexposure to antigen, providing protection against previously encountered pathogens (56, 57). Therefore, an effective antibody-based vaccine must stimulate production of antigen-specific LLPC. We tested the ability of the MPER/liposome formulation to generate LLPC and characterized this population at the single-cell level. To this end, BALB/c mice were immunized three times at 21-day intervals with the MPER anchored to the liposome membrane via a covalently attached N-terminal palmitoyl adduct. The liposomes were previously optimized (41, 42) to trigger humoral responses by including the Toll-like receptor 4 (TLR4) agonist MPLA as an adjuvant and the I-A^d-presented T cell epitope LACK1, the immunodominant peptide of the *Leishmania major* LACK protein, to stimulate CD4 T cell help (58). Following immunization, sera were drawn from mice and endpoint titers for IgG isotype antibody binding to MPER/liposomes determined by direct ELISA. ELISA revealed that MPER-specific antibody endpoint titers of approximately 80,000 were maintained for up to 180 days following the third immunization (Fig. 1A). Since we previously showed that MPER/liposome immunizations result in dominant antibody responses directed to the C-terminal helix of the MPER, including the free amide exposed on the C-terminal end of the MPER sequence following synthesis (K683) (42), we also determined the magnitude of the serum antibody responses independent of the free amide in binding specificity by using MPER-COOH peptides. The analysis revealed that non-amide-reactive MPER-specific serum antibody responses were durably maintained by LLPC as well, albeit at 8 times lower titers.

Next, we determined the frequency of ASCs in BM over time following the third immunization. By coating 96-well PVDF membrane plates with MPER/liposomes and then incubating BM cells on the membranes overnight, the ASCs were visualized and quantified by ELISPOT assay, analogously to the procedures employed for soluble protein antigens. Consistent with the serum endpoint titer results, the majority of MPER-specific ASCs (50/10^6 cells to 100/10^6 cells) were of the switched IgG isotype, particularly IgG1; however, ~10 MPER-specific ASCs/10^6 cells of each of the IgM, IgG2a, IgG2b, and IgG3 isotypes were also maintained for up to 180 days (Fig. 1B). The same trend was also observed with MPER-specific BM plasma cells after the second immunization (data not shown). To assess the relative affinities of antibodies produced by ASCs in BM for the MPER following the third immunization, we developed a simple assay based on ligand display. We reasoned that a low-affinity antibody would not bind to MPER/liposomes in which the MPER was presented at a low density (1:1,000 peptide:lipid ratio) versus the higher density (1:50 ratio) used for total ASC quantification. The use of lower-density MPER in the liposome array (1:1,000 ratio) to exclusively detect high-affinity antibodies was validated by control experiments using representative high- and low-affinity rMAbs (113 and 196, respectively) elicited by MPER/liposome immunization and by comparison with the high-affinity 2F5 and 4E10 BNAbs (Fig. 1C). In addition, as shown subsequently, the relative binding affinities of rMAbs 113 and 196 were 3,400 response units (RU) and 380 RU, respectively, for MPER/liposomes at 30 μg/ml as measured by surface plasmon resonance (SPR) (see Fig. 4A). Parallel analysis at various MPER:lipid density ratios (1:50 to 1:1,000) by ELISA revealed that 2F5, 4E10, and the high-affinity clone 113 bound well. In contrast, the low-affinity clone 196 antibody bound to MPER/liposomes at the 1:50 ratio with a high signal but had little reac-

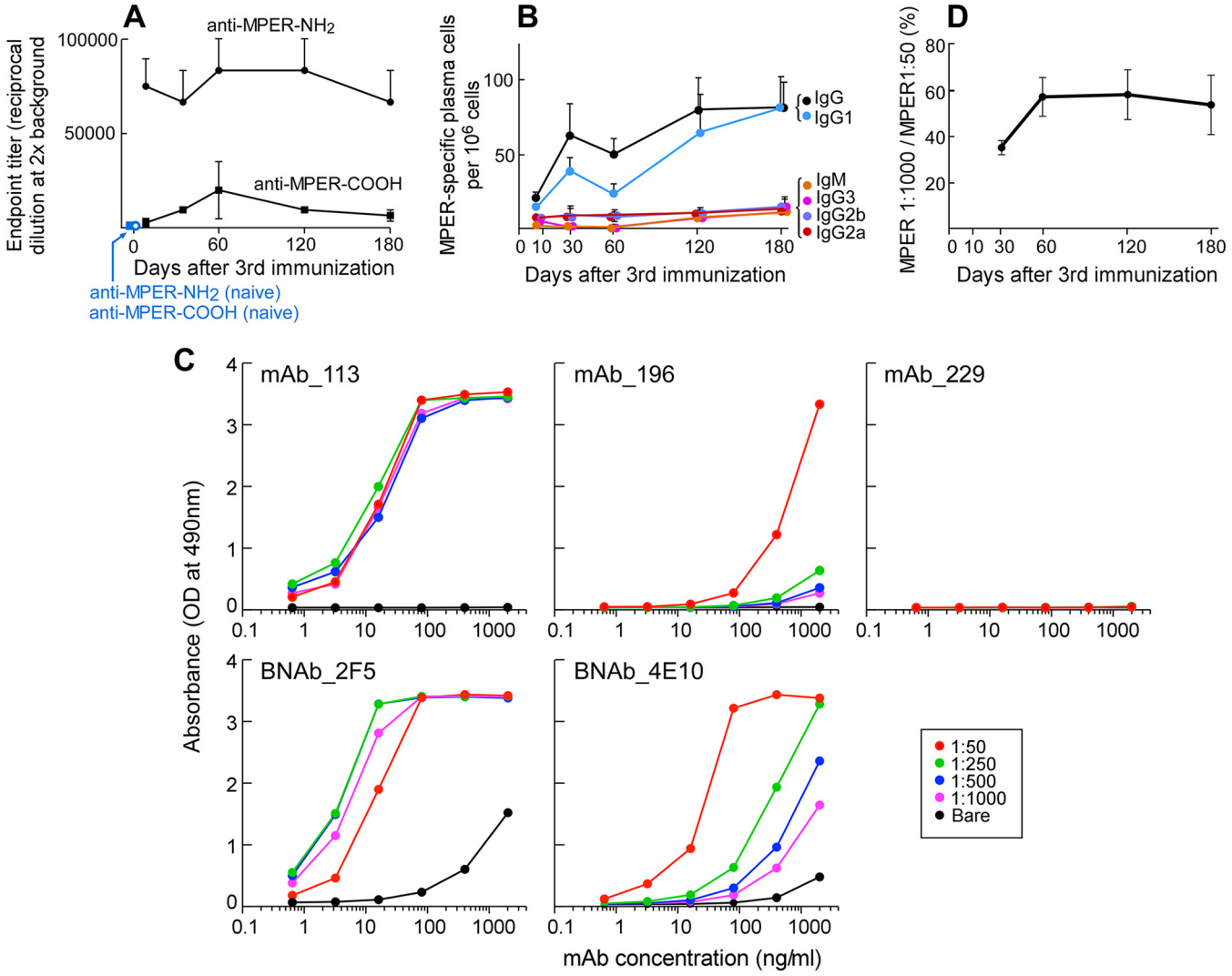

FIG 1 MPER/liposome immunization results in long-term, MPER-specific, isotype-switched antibody responses. (A) Endpoint titers of MPER-NH_2/liposome (circles)- and MPER-COOH/liposome (squares)-specific IgGs were measured by ELISA at the indicated time points after the third immunization. Control data from naive mice are shown with blue circles (anti-MPER-NH_2/liposomes) and squares (anti-MPER-COOH/liposomes). (B) Kinetics of MPER-binding and isotype-specific ASCs elicited after the third immunization. Numbers of MPER-binding ASCs from BM were determined by ELISPOT assay, using MPER-NH_2/liposomes as the capture antigen. Quantification of numbers of anti-MPER-specific ASCs per 10^6 bone marrow cells was performed by ELISPOT assay at the indicated time points. Secretion of immunoglobulin was assessed by specific isotype. Symbol colors: black, IgG; blue, IgG1; orange, IgM; pink, IgG3; purple, IG2b; red, IgG2a. (C) Low-affinity (196) but not high-affinity (113) rMAbs are sensitive to the copy number of MPER segments arrayed on the surface of a liposome. ELISA plates coated with streptavidin were incubated with liposomes containing biotin-PEG 2000 as well as MPER at peptide:lipid ratios of 1:50 (red), 1:250 (green), 1:500 (blue), and 1:1,000 (purple) or with bare liposomes (black). All serially diluted Abs (from 2 μg/ml to 64 pg/ml) were incubated on liposomes overnight and developed with anti-human secondary antibody. Points shown represent means for duplicate analyses. High-affinity BNAbs 2F5 and 4E10 were compared as positive controls, and irrelevant rMAb 229 was used as a negative control. (D) Relative affinities of MPER-binding IgG BM ASCs at different time points as assessed by ELISPOT assay. The frequencies of low-density MPER/liposome (1:1,000 [mol:mol])- and high-density MPER/liposome (1:50)-binding IgG ASCs were determined, and the ratios of low-density MPER (1:1,000) to high-density MPER (1:50) binding were plotted. All points in panels A, B, and D are means ± standard errors of the means (SEM) for quantification of data from 3 independent mice at each time point for ELISA and ELISPOT assays. Representative data are shown. All graphs represent BALB/c mice immunized with Npalm-MPER/liposomes loaded with a LACK1 T cell helper peptide and MPLA as an adjuvant, administered by intradermal injections on three occasions at 3-week intervals.

tivity to those at ratios at or below 1:250 (Fig. 1C). Quantification of the numbers of cells binding the MPER/liposomes at 1:1,000 (low ratio) versus the high ratio (1:50) by ELISPOT analysis revealed that the percentage of cells binding both MPER/liposomes at 1:1,000 and MPER/liposomes at 1:50 reached and was maintained at nearly 60% by 60 days after the third immunization (Fig. 1D). These analyses indicate that the MPER-specific IgG-producing LLPC in BM are associated with the persistent MPER-specific antibody responses in serum. Moreover, not all MPER-specific LLPC in BM produce high-affinity Abs (e.g., rMAb clone 196 has a low affinity) (Fig. 1C).

Isolation of single MPER-specific LLPC by microengraving. We next sought to characterize the variable (V), diversity (D), and joining (J) gene segments of immunoglobulins elicited by MPER/liposomes by using DNA sequencing at the single-cell level. This approach allowed us to determine the diversity of B cells recruited

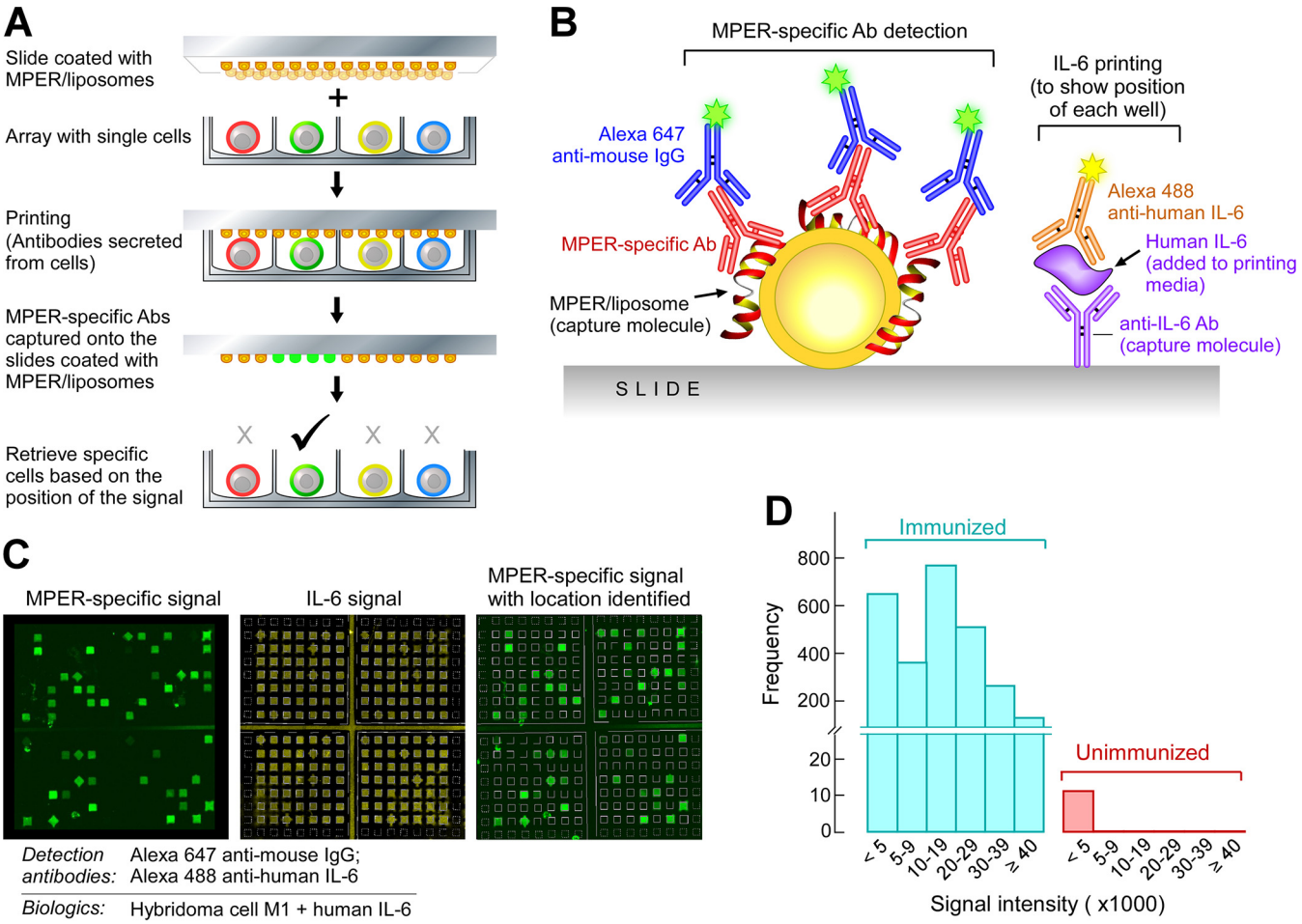

FIG 2 Identification and isolation of single MPER-specific BM plasma cells by use of microengraving technology. (A) Diagram of the microengraving method. (B) Interrogation of slides after printing. MPER-specific Abs captured on MPER/liposome-coated slides were detected with Alexa 647-conjugated anti-mouse IgG. Human IL-6 was detected with Alexa 488-conjugated anti-human IL-6 to produce signals in every well for grid alignment and localization of MPER-specific signals. Human IL-6 was added to the printing medium. (C) Establishment of the microengraving system by using MPER-specific M1 hybridoma cells. The MPER-specific signals (green squares) were overlaid on the IL-6 signals (yellow squares) for localization of MPER-specific cells and retrieval for analysis. The MPER-specific M1 hybridoma cell line was used as an example. (D) Detection of MPER-specific plasma cells from bone marrow. Plasma cells were isolated from BM by depleting $B220^+$ cells and $CD49b^+$ cells and then enriching for $CD138^+$ cells. A total of 2,674 MPER-specific signals were detected from 70,000 BM plasma cells isolated from one mouse immunized with Npalm-MPER/liposomes, whereas only 11 signals, all with signal intensities of <5,000, were detected from an unimmunized mouse.

as components of the anti-MPER response by the extent to which these cells underwent somatic hypermutation (SHM) and then through recombinant protein expression to define the molecular characteristics, including CDR3 lengths, important for MPER binding. To identify and isolate MPER-specific LLPC, we took advantage of the versatile microengraving technology, which uses a dense array of microwells (0.1 to 1 nl each) containing individual cells to print a corresponding array of antibodies secreted by each cell (59, 60). Microengraving is performed by distributing cells on an injection mold containing grids of microwells and exposing the wells to an antigen-coated slide. In detail, plasma cells were purified from mouse BM cells 10 days after the third immunization with various MPER/liposome formulations, resuspended in medium containing human IL-6 to mark the grid, and distributed onto an array of microwells in a poly(dimethylsiloxane)-injected mold to allow the analysis of ~100,000 total cells per array (Fig. 2A). A glass slide coated with MPER/liposomes (1:50 MPER:lipid ratio) and anti-human IL-6 was placed over the wells. The slide-mold arrangement was clamped into position and incubated for 1 h to allow secreted antibodies to bind to MPER/liposomes, while the IL-6 was bound by the coprinted anti-IL-6 capture antibody (Fig. 2B). M1 hybridoma cells producing MPER-specific antibody were tested as a positive control to demonstrate the lucidity of the method for localizing wells with MPER-specific cells (Fig. 2C, left panel). After incubation, the slide was removed, and Alexa 488-labeled anti-IL-6 was used to visualize the grid of the mold (Fig. 2C, middle panel, yellow wells). The MPER-specific antibody was detected with Alexa 647-labeled anti-mouse IgG, and this signal (shown in green) was overlaid on the IL-6 signal so that wells containing MPER-specific cells could be located (Fig. 2C, right panel). The cells were binned by their supernatants' MPER antibody detection signal intensities (Fig. 2D) and were retrieved by use of a micromanipulator for reverse transcription-PCR (RT-PCR).

The frequencies of MPER-specific plasma cells in BM 10 days after the third immunization with Npalm-MPER/liposomes

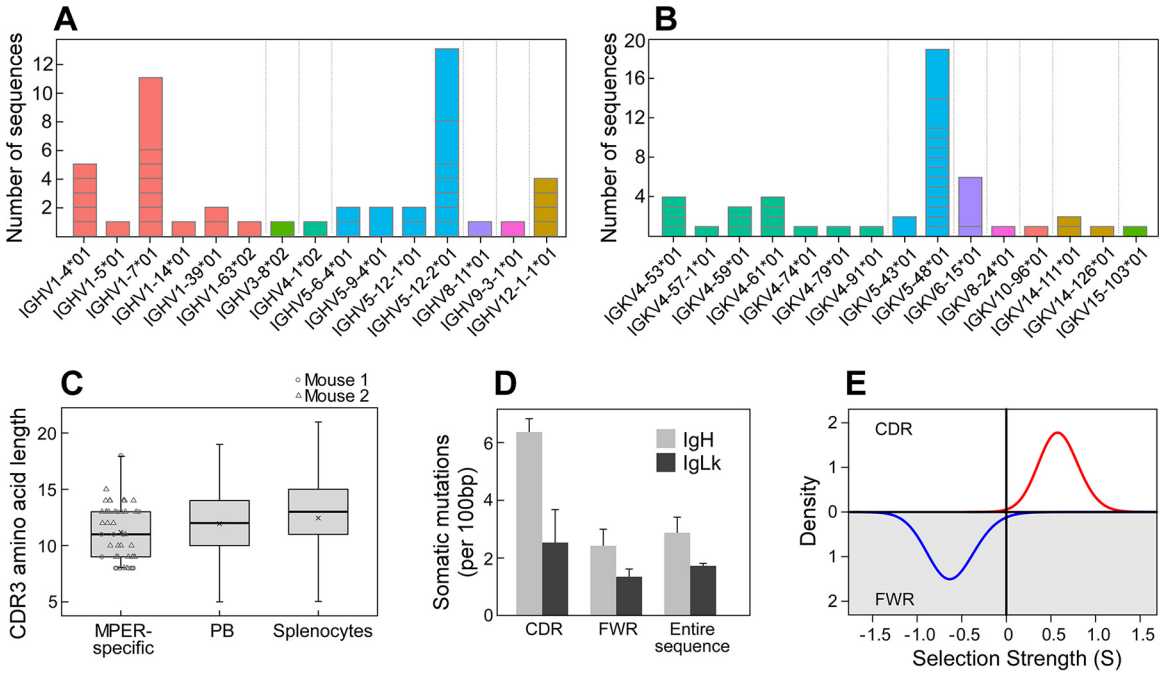

FIG 3 Immunoglobulin gene usage within the MPER-specific bone marrow plasma cell population is diverse. Immunoglobulin genes from two mice ($n = 66$ total sequences generated; 48 sequences were analyzed) were amplified from single MPER-specific IgG-secreting plasma cells. The usage frequencies of immunoglobulin V_H genes (IGHV) (A) and V_L genes (IGKV) (B) are diverse. V gene families were defined using IMGT and color coded by gene family. The number of sequences representing each IGHV and IGKV family is shown, with horizontal gray lines separating groups of clonally related sequences within each V gene cohort. (C) Box plot of CDRH3 length distributions. CDRH3 regions were identified by IMGT, and amino acid lengths were calculated. Each point represents a sequence from mouse 1 (circles) or mouse 2 (triangles). For comparison, mouse CDRH3 lengths for IgG sequences from splenocytes or plasmablasts (PB) are shown, using previously published data (76). Note that a single outlier point for mouse splenocytes is not shown. The mean value for each group is marked with a cross. (D) The number of somatic mutations per 100 germ line-defined base pairs was calculated for the CDRs, the FWRs, and the entire sequence of the IgH (gray columns) and IgLk (black columns) V genes. (E) BASELINe analysis of selection pressure on IgH V gene sequences. Significant positive selection was calculated for nonsynonymous CDR mutations ($\Sigma = 0.59$; $P = 0.005$; red line), along with significant negative selection against nonsynonymous mutations in the FWR region ($\Sigma = -0.62$; $P = 0.015$; blue line). The data represent analyses of sequences from two independent B cell/immunoglobulin gene isolations by microengraving.

ranged from ~1.5 to 3% of total plasma cells by microengraving; the results of one representative experiment are shown in Fig. 2D. Only 10 to 20 cells from an immunologically naive mouse were scored positive, but with signal intensities of <5,000 (Fig. 2D).

Genetic characterization of MPER-specific Ig repertoires. BNAbs to HIV have been typified by long CDRH3 sequences and high mutation frequencies (6, 61), with the antibody responses to some epitopes dominated by particular VH genes, such as the well-defined prevalence of VH1-2 among the CD4-binding site agonist antibodies (62–65). To investigate the genetic composition of the MPER-specific Ig repertoires, RT-PCR was utilized to amplify variable regions of naturally paired IgH and IgLk antibodies by using a strategy previously described by Tiller et al. (53). Immunoglobulin genes from two mice immunized with Npalm-MPER/liposomes were amplified from single MPER-specific IgG-secreting plasma cells. The sequences ($n = 66$ total sequences generated) were aligned by use of IMGT/HighV-QUEST (version 1.5.1) to identify their V(D)J germ line segments. Sequences for which a junction could not be identified ($n = 18$) were excluded from further analyses, leaving 15 sequences for mouse 1 and 33 for mouse 2. The MPER-specific immunoglobulin repertoires were derived from a diverse collection of gene families for both the V_H (IgH V gene) (Fig. 3A) and V_L (IgLk V gene) regions (Fig. 3B), some of which were clonally expanded. As shown in Fig. 3C, the sequences also used a diverse set of CDRH3 lengths, which fell within the range of expected lengths for mice. Virtually all of the sequences (94%) showed somatic hypermutation, with averages of 2.9 and 1.7 mutations/100 bases for V_H and V_L, respectively, and with a higher frequency of mutations in the CDRs (Fig. 3D). To determine whether these mutation patterns were driven by affinity maturation, we quantified selection strength (Σ) by using the BASELINe method (55). Positive values for Σ reflect a higher incidence of nonsynonymous mutations than expected and are associated with positive selective pressure, while negative values for Σ reflect a higher incidence of synonymous mutations than expected and are associated with negative selection pressure. BASELINe analysis revealed significant evidence for positive selection in the CDR, as expected for antigen-driven affinity maturation ($\Sigma = 0.59$; $P = 0.005$). In addition, there was significant negative selection in the framework regions (FWR), as expected to preserve the overall antibody structure ($\Sigma = -0.62$; $P = 0.015$) (Fig. 3E). Thus, the MPER-specific Ig repertoires reflect a diverse, affinity-matured cell population.

Residue-specific binding analysis of rMAbs reveals common epitope recognition with diverse functional characteristics. We next selected a representative group of matched IgH/IgLk sequences that included CDRH3 lengths across the range of 5 to 19 amino acids and sequences representing diverse gene families. A total of 20 rMAb clones were selected for expression and characterization by cloning of the selected amplicons into IgH/IgLk ex-

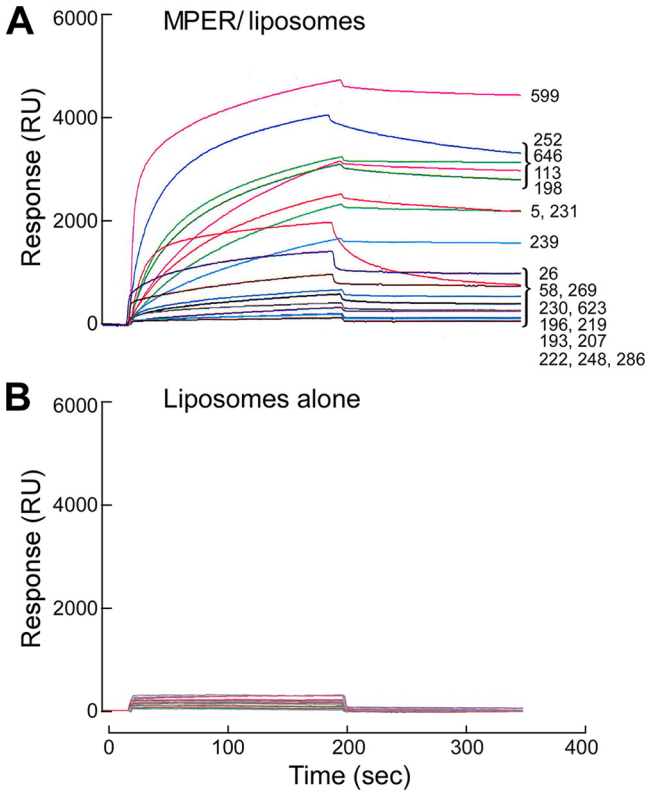

FIG 4 Binding specificities of rMAbs analyzed by SPR analysis. Results are shown for 20 rMAbs binding to MPER/liposomes (DOPC/DOPG) (A) and to liposomes only (B). The scale bars have been equalized to demonstrate the clear specificity for the MPER. Each purified rMAb was tested at 30 μg/ml by injection over L1 chip-bound MPER/liposomes or liposomes only at a flow rate of 10 μl/min for 3 min.

pression vectors as described previously (53). The purified rMAbs were then confirmed to have MPER specificity by SPR analysis. Figure 4A and B show relative binding affinities of 20 rMAbs for the MPER arrayed on the surfaces of MPER/liposomes and for liposomes alone. Although LLPC are high-affinity antibody producers, not all MPER-specific rMAbs appear to be high affinity by qualitative measures, as exemplified in Fig. 4A and 1C. While several antibodies showed modest binding reactivity to liposomes alone, the majority of rMAbs had no or weak lipid binding, with no direct correlation to the affinity of the Abs for MPER.

To determine the fine epitope specificity of the rMAbs, we performed SPR binding analysis using a panel of single alanine mutants comprising each of the 22 MPER amino acids. Given that an amide group at the C terminus of the MPER was critical for antibody binding in polyclonal immune sera (42), an MPER-COOH construct was also included to evaluate the binding contribution of the amide. The binding reactivities of all 20 purified rMAbs were reduced by MPER-COOH mutation, indicating that all rMAbs recognized the C-terminal helix of the MPER. Based on the hierarchy of relative binding affinities (Fig. 4A) and the genetic usage of the 20 rMAbs tested, further fine epitope mapping was performed on a collection of 12 rMAbs. As shown in Fig. 5A for the representative set of 12 rMAbs, a conserved antibody binding footprint was observed, requiring S668, N677, W680, and the C-terminal amide in MPER. However, for W672, F673, N674, I675, and L679, each specific residue's contribution to binding differed somewhat between antibodies. Overall, the rMAbs showed fine epitope specificities similar to but distinct from those of 4E10 and 10E8 (6, 12). In addition, with the exception of clones 599 and 646, V_H and V_L gene usages suggested that all were derived from different germ line B cell lineages with different CDRH3 lengths, ranging from 8 to 15 residues (Fig. 5B), demonstrating that a surprising amount of gene diversity can lead to a conserved MPER epitope specificity.

As an orthogonal approach, we screened the ASCs for epitope specificity by ELISPOT assay. Besides the MPER-COOH mutant noted above, we designed a second amide-lacking variant with a W680A mutation (W680A-COOH). Further, we included two truncated MPER peptides. One, termed MPER-N, contained the amino acids from E662 to T676, and the second, termed MPER-C, included amino acids A667 to K683, comprising the nominal 10E8 binding site. All five of these peptides were N-terminally palmitoylated for ease of incorporation into liposomes. We arrayed them on liposomes and screened ASCs from BM, inguinal lymph nodes (iLN), and spleens for reactivity 5 days after the initial booster immunization with Npalm-MPER/liposomes (Fig. 5C). The MPER-NH_2 variant, which was the immunogen, represented the most frequent ASC specificity (~50 iLN, ~100 spleen, and ~75 BM ASCs/10^6 cells) (Fig. 5C). On the other hand, MPER-COOH and W680A-COOH captured antibodies from ASCs at significantly lower frequencies (~5 iLN, ~25 spleen, and ~20 BM ASCs/10^6 cells for MPER-COOH and ~0 iLN, ~25 spleen, and ~10 BM ASCs/10^6 cells for W680A-COOH). Furthermore, while MPER-N was not bound by antibodies from ASCs in the iLN, spleen, or BM, the MPER-C was bound. Taken together, these results indicate that although weak, a small fraction of Abs recognize the C-terminal region of MPER independently of the NH_2 group, and the results are consistent with the antibody titer against MPER-COOH detected in serum (Fig. 1A).

MPER/liposome immunizations do not generate polyreactivity to cardiolipin and dsDNA. MPER-specific BNAbs, such as 2F5 and 4E10, have long CDRH3 and have been found to be polyreactive. In addition, both the lipid-integrated nature of the MPER and the amino acid sequence of the MPER shared with some parts of autologous proteins (kynureninase and splicing factor 3B subunit 3) have been proposed to make the MPER stealthy to all but nonpolyreactive antibodies (47). Given that the MPER/liposome-elicited rMAbs all displayed a common binding footprint, but with distinct genetic and biochemical properties, including CDRH3 length (Fig. 5), we reasoned that if polyreactivity were the characteristic of MPER-specific Abs, many antibodies with long CDRH3 would bind to standard model targets, such as cardiolipin and/or dsDNA. In addition to the 20 rMAbs generated with the Npalm-MPER immunogen, another 22 rMAbs, generated from MPER mutant Npalm-W680A/liposome and MPER-Cpalm/liposome (MPER palmitoylated at the C terminus) immunizations, were also tested for cardiolipin and dsDNA reactivity and compared with 2F5, 4E10, and 10E8. Notably, most antibodies (39/44 rMAbs) tested did not bind either cardiolipin or dsDNA (Fig. 6A), including three rMAbs elicited with the MPER mutant Npalm-W680A/liposome immunization, which exhibited 2F5-like epitope specificity. Among the 20 rMAbs characterized in Fig. 4 and 5, four antibodies (198, 207, 219, and 193) were polyreactive. The epitope specificities of antibodies 198 and 230 were distinct but were most similar to that of 10E8 (Fig. 5A), with only

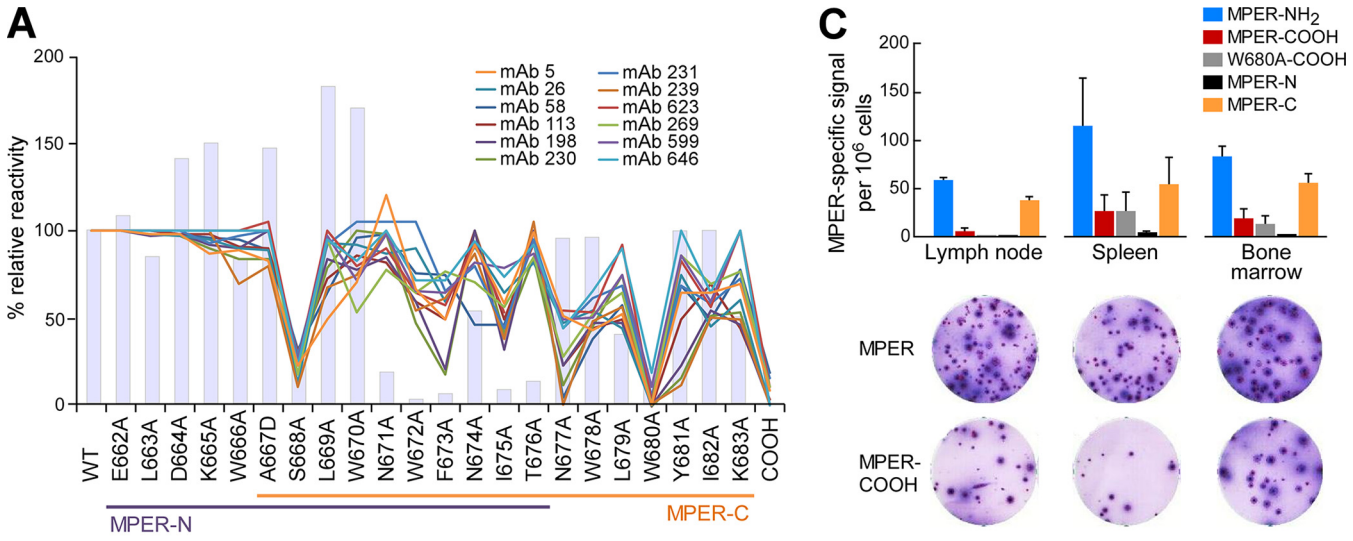

B

mAb ID	Heavy chain: VDJ gene usage VH	D	JH	CDR3 Length	CDR3 Sequence	Light chain: VJ gene usage VK	JK	CDR3 Length	CDR3 Sequence
58	5-9-4	2-13	1	13	ARGGLDPYYFDVW	5-43	2	9	QQSNRWPHT
113	5-12-1	1-1	2	11	ARGGTTEAFDY	5-48	5	9	QQSNGWPTT
230	3-8	1-2	2	15	ARYRKYYGWEYYFDY	14-126	5	9	LQHGESPLT
198	12-1-1	4-1	4	10	SREKNWEMDY	4-53	4	9	QQWSGYPVT
26	5-12-2	2-4	4	11	ARQGITEPMDY	5-48	1	9	QQGYGWPTT
239	1-39	1-1	2	13	ARNYYGSSFHFDY	4-61	2	10	QQYHSYPPIT
231	9-3-1	2-14	3	12	ARRGEVRRWFAY	10-96	1	9	QQGNTLPWT
623	2-2	3-1	4	12	ARKQFGYYDMDY	3-5	1	9	QQSNEDPWT
269	5-12-2	1-1	2	14	ARLRGPTVVVPFDY	5-48	1	9	QQSYGWPTT
599	5-4	1-1	2	11	ARQGITYGHDY	4-57	5	9	LQRTSYPLT
646	5-4	1-1	2	11	ARGGINYGHDY	4-57	5	9	QQRTSYPLT
5	1-7	2-3	2	8	SRQGLMNY	5-48	5	9	QQSYGWPTT

FIG 5 rMAb epitope mapping analysis reveals convergence to a common epitope at the C-terminal region of the MPER and use of various CDRH3 lengths. (A) Epitope specificity analysis by BIAcore of 12 representative rMAbs by use of liposome-bound serial single alanine MPER mutants. The *y* axis shows the percent relative binding activities of Abs against each single-residue mutant compared to that of wild-type MPER (WT) (100%). Colored lines represent the epitope specificities of MPER/liposome immunization-derived antibodies, and bars represent the BNAb 10E8. (B) IgH (blue table) and IgLk (green table) V(D)J gene usage and CDR3 analysis of the 12 representative rMAbs from panel A. The germ line gene segment usage, CDR3 lengths, and sequences of the MPER-specific Abs were determined via IMGT/HighV-QUEST analysis. (C) Frequencies of MPER-specific ASCs with different specificities in various organs 5 days after the second immunization with Npalm-MPER/liposomes. Numbers of MPER-binding ASCs were determined by ELISPOT assay, using each of the different epitope-specific MPER/liposomes as the capture antigen. MPER-NH_2 and MPER-COOH indicate the HXB2 MPER with C-terminal NH_2 and COOH ends, respectively, and W680A-COOH indicates a W680 mutation to A with a C-terminal COOH. The MPER-N (E662 to T676) and MPER-C (A667 to K683) sequences are indicated in panel A.

antibody 198 manifesting cardiolipin binding. The rMAbs 198 and 207 bound cardiolipin similarly to the BNAb 2F5 but half as well as antibodies 650 and 219 at 5 μg/ml. Antibodies 650 and 219 also bound dsDNA at concentrations down to 0.1 μg/ml and 1 μg/ml, respectively, while rMAb 193 joined them, with dsDNA sensitivity at concentrations down to 1 μg/ml. All five of these rMAbs recognized the C-terminal helix of MPER. The five antibodies that showed polyreactivity (650, 219, 198, 207, and 193) had CDRH3 lengths ranging from 5 to 14 residues. Although a long CDRH3 loop has been associated with polyreactivity (66), no correlation between polyreactivity and the length of the CDRH3 loop was observed in this study (Fig. 6B).

The CDRH3 loops of MPER-specific antibodies reveal dissociable antigen specificity and polyspecificity properties. To further define the dual reactivity of MPER-specific Abs, we evaluated the biochemical properties of the antigen combining sites of two different sets of antibodies. Clones 198 and 252 shared the same V_H gene and J_H gene segments (HV12-1/HJ4) and IgLk V_L gene usage (KV4-53) but differed in their J_L gene usage (KJ4 versus KJ5, respectively) (Fig. 7A). These clones utilized different D gene segments, resulting in very different CDRH3 sequences (SREKNWEMDY for clone 198 and SRENPKIYYALDY for clone 252). Interestingly, the binding properties of these two clones also varied significantly. Clone 252 bound MPER/liposomes with a higher on-rate and a higher overall response than those of clone 198 by SPR analysis (Fig. 7B), but by ELISA, clone 198 bound the lipid cardiolipin, while clone 252 binding was barely detected (Fig. 7C). Therefore, clone 198 reactivity manifested both MPER-specific

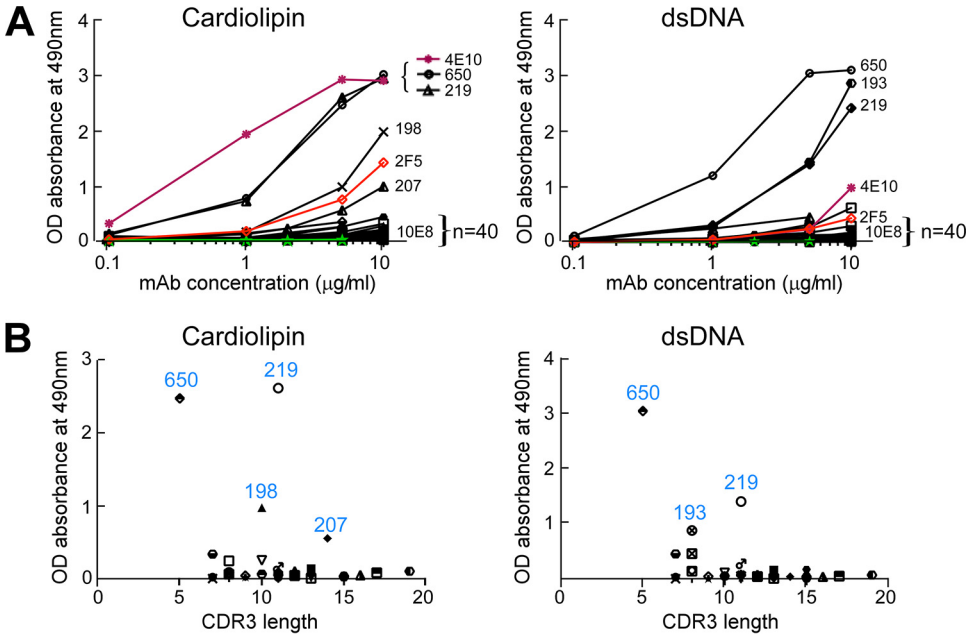

FIG 6 Low frequencies of autoreactivity and polyreactivity of MPER-specific Abs elicited by immunization with various MPER/liposome vaccines. (A) Forty-four different MPER-specific rMAbs from mice immunized with liposome vaccines containing Npalm-MPER, the Npalm-W680A mutant, or Cpalm-MPER were tested for autoreactivity and polyreactivity by cardiolipin and dsDNA ELISAs and were compared with anti-MPER BNAbs (red, 2F5; purple, 4E10; and green, 10E8). Data shown are representative of three independent experiments. (B) Lack of correlation between reactivities and CDRH3 lengths among the 44 different Abs tested in panel A. The *y* axis represents the absorbance at 490 nm of bound antibodies from panel A at 5 μg/ml, plotted against CDRH3 length on the *x* axis.

reactivity and polyreactivity, while clone 252 was MPER specific and lacked polyreactivity (Fig. 6A and 7C). The DOPC/DOPG liposome binding of both clones 198 and 252 was weak (Fig. 7B, right panel), and this trend was supported by negligible reactivity of either clone to dsDNA (Fig. 7C). As shown in Fig. 7B (left panel), when the IgH of clone 252 was paired with the IgLk of clone 198 (252H/198K chimera), binding to MPER was dramatically reduced, with only ~30% residual binding reactivity relative to that of the clone 252 parent IgG pair. Similar results were shown with 198H/252K chimera binding to the MPER relative to that of clone 198. Next, the chimeric rMAb 252M was made by swapping the CDRH3 of clone 252 with that of clone 198 to determine the critical role of CDRH3 for antigen specificity. Swapping of the CDRH3 of clone 198 with that of clone 252 resulted in the abrogation of 252M binding to MPER/liposomes as determined by SPR analysis (Fig. 7B, middle panel). On the other hand, 252M bound cardiolipin with 3 times the absorbance of its parent CDRH3-containing rMAb 198 and with 10 times the absorbance of clone 252 at a concentration of 5 μg/ml (Fig. 7C). Similar to clones 198 and 252, the chimeric Ab 252M did not have dsDNA reactivity (Fig. 7C). Note that nonspecific liposome binding (DOPC/DOPG) of 252M was also increased compared to that of clones 252 and 198 (Fig. 7B, right panel). As shown in Fig. 8A, the sequences of clone 252 IgL and clone 198 IgL differ by 5 amino acid residues. Two of these residues are relatively homologous, i.e., M94 (clone 252)/V94 (clone 198) in the FR3 region and L112/V112 near the end of the CDRL3 loop, and probably have little effect on MPER binding. H38/N38 is in the CDRL1 loop, which may contact the MPER, and L40/H40 in FR2 is buried but adjacent to the CDRH3 loop (Fig. 8B). It is possible that these two residues influence the conformation of the CDRH3 loop, resulting in the reduced MPER binding observed with the 198H/252K and 252H/198K chimeras (Fig. 7B, right panel). The fifth residue, N66/K66, located at the beginning of the FR3 region, is also in the vicinity of the CDRH3 loop and may play a minor role. The CDRH3 loop in clone 198 contains a tryptophan residue at its apex that confers better membrane binding than that with the CDRH3 loop in clone 252. Interestingly, membrane binding of 252M increased significantly even compared to that of wild-type clone 198, which has the same CDRH3 loop (Fig. 7B, right panel). It is possible that the identical CDRH3 loops in these two constructs adopt different conformations as a result of neighboring residues or that the approach angles of the antibodies with respect to the membrane are different. Notwithstanding this possibility, membrane binding and cardiolipin binding were uncorrelated with MPER binding for the wild-type clones 198 and 252 and the CDRH3 loop-swapped mutant 252M.

In a second set of clones, 196 and 219, a trend toward a reverse correlation between MPER binding and polyreactivity was determined by chain swap and/or CDRH3 mutations in the antibody combining site. Clones 196 and 219 share the same V_L/J_L gene pairings (KV3-1/KJ1) and have different V_H/J_H gene pairings (HV5-6-5/HJ3 and HV5-6-5/HJ4) (Fig. 9A), and they differ by 13 IgH and 5 IgLk amino acids. As shown in Fig. 9B, mispairing of IgH and IgLk of clone 196 with those of clone 219 reduced MPER/liposome binding compared to that of clone 196 (left panel). Replacement of clone 219 CDRH3 with that of clone 196 to create a new clone, 219M, greatly increased the MPER/liposome on-rate and total binding (Fig. 9B, middle panel). However, this enhanced MPER/liposome binding was almost entirely due to a nonspecific lipid binding contribution (Fig. 9B, right panel). Along with increased cardiolipin and dsDNA binding by 219M (Fig. 9C), these results suggest that the 196 and 219 antibodies affinity matured toward MPER specificity independently of polyreactivity.

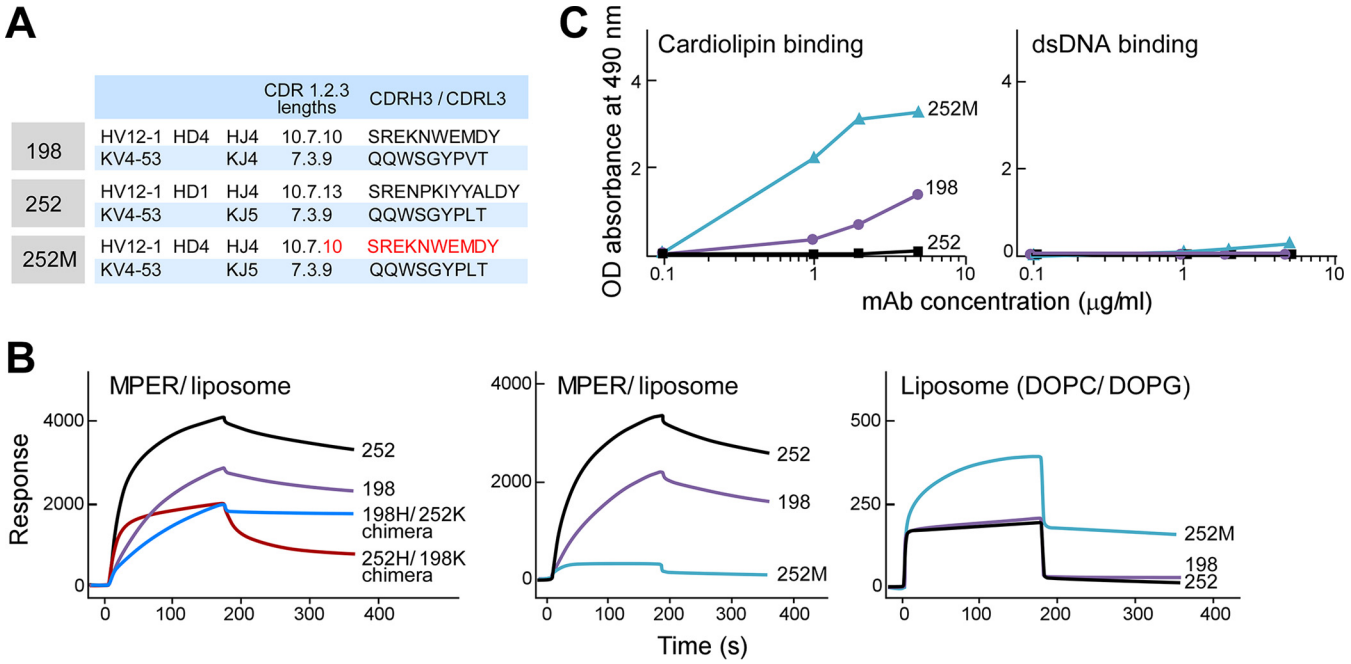

FIG 7 The CDRH3 loop plays a critical role in MPER specificity versus polyspecificity. (A) IgH and IgLk V(D)J gene usage of the related Abs 198 and 252. 252M is a 252 variant in which CDRH3 of clone 252 was replaced by CDRH3 of clone 198. (B) Relative binding affinities of chimeric rMAbs for MPER/liposomes compared to those of WT clones 198 and 252 as measured by SPR analysis (left), binding reactivities of 252M for MPER/liposomes in comparison to those of WT clones 198 and 252 (middle), and lipid-binding reactivities of clones 198, 252, and 252M (right). (C) rMAbs were tested for polyreactivity by cardiolipin and dsDNA ELISAs.

DISCUSSION

Previously, we characterized the polyclonal immune serum responses of BALB/c mice elicited against an MPER/liposome vaccine incorporating molecular adjuvants and CD4 T cell help (41, 42). In the present study, we focused on defining the LLPC in BM that are responsible for that serum antibody production. The implementation of microengraving methods to assess MPER/liposome specificity at the level of single plasma cells allowed us to

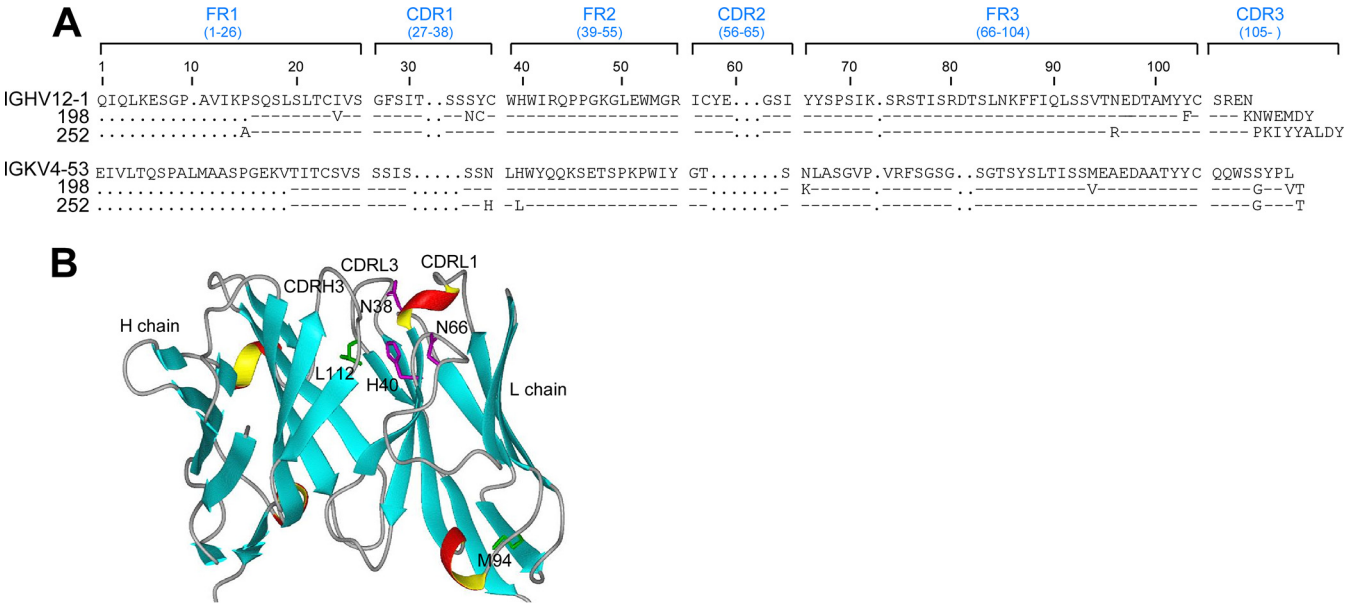

FIG 8 Comparison of rMAbs 198 and 252. (A) Amino acid residue alignments of rMAbs 198 and 252. (B) Modeling of rMAb 198 with predicted IgLk residue differences from rMAb 252. Residues N/H38, H/L40, K/N66, V/M94, and V/L112 were modeled on an immunoglobulin variable region ribbon structure (heavy chain [PDB entry 1ACY] and light chain [PDB entry 5D8J], with homologous sequences). Residues V94 and V112, within FR3 and CDRL3, respectively, are illustrated as the homologous residues M94 and L112 in rMAb 252. Note that N38 and H40, located in CDRL1 and FR2, respectively, are adjacent to the CDRH3 and are replaced by H38 and L40 in rMAb 252. As illustrated, residue N66 at the beginning of FR3 is also near CDRL3 and is K66 in rMAb 198.

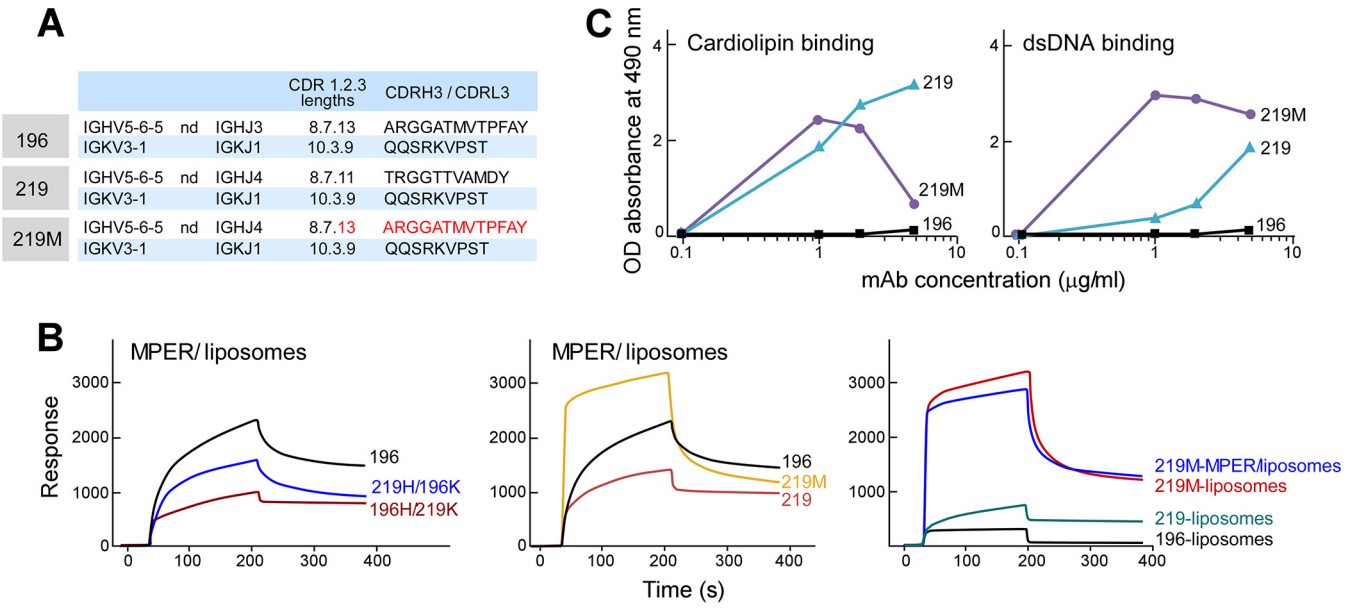

FIG 9 Reverse correlation between MPER binding and polyreactivity determined by chain swap and/or CDRH3 mutations. (A) IgH and IgLk V(D)J gene usage of related Abs 196 and 219. 219M is a 219 variant in which CDRH3 of clone 219 was replaced by CDRH3 of clone 196. (B) Relative binding reactivities to MPER/liposomes as assessed by SPR analysis of chimeric rMAbs from clones 196 and 219 compared to that of naturally paired clone 196 (left panel). Also shown are 219M binding reactivities for MPER/liposomes (middle) and liposomes only (right) in comparison to those of WT clones 196 and 219. Thirty microliters of each antibody at 100 μg/ml was injected over the MPER/liposome or liposome surface of an L1 chip at a flow rate of 10 μl/min for 3 min. (C) rMAbs were tested for polyreactivity by cardiolipin and dsDNA ELISAs.

investigate their immunoglobulin V_H and V_L gene usage and to characterize representative rMAbs to elucidate the immunogenicity of MPER/liposomes in finer detail. Utilizing liposome-arrayed MPER immunogens, we observed that the majority of MPER-specific LLPC in BM produce antibodies directed to the C-terminal helix of the MPER region and exhibit evidence of affinity maturation (Fig. 3, 5, and 7). These results imply that these antibodies represent polyclonal immune responses elicited in sera by use of Npalm-MPER/liposomes, as described previously (42). It is evident that LLPC are derived mainly from memory B cells after booster immunization, as they are minimally, if at all, detectable after primary vaccination but readily evident, both serologically and by ELISPOT assay, following booster immunization (Fig. 1 and 5; data not shown). B cell repertoire analysis (Fig. 3) in conjunction with epitope mapping of rMAbs (Fig. 5) collectively indicated that a prominent common epitope specificity is generated by utilization of a variety of different germ line genes. This recognition of antigen follows independent B lineage pathways through affinity maturation, exploiting the structural plasticity of the antigen combining site to achieve this common goal.

Antibody binding to cardiolipin, dsDNA, or Hep-2 cells is commonly measured to assess polyreactivity or autoreactivity. As shown in Fig. 6, only 5 of 44 MPER-specific rMAbs generated by various MPER/liposome vaccines were polyreactive and/or autoreactive. No clear correlation was observed between the CDRH3 length and polyreactivity among the tested mouse MPER-specific antibodies, nor was there an association of polyreactivity with a particular V gene family encoding IgH or IgLk variable regions. When CDRH3 of rMAb 252 was replaced with that of the genetically related clone 198 to create 252M, the MPER epitope specificity was abrogated. Conversely, the 252M reactivities for both cardiolipin and dsDNA were increased compared to those of clone 252. Note that polyreactivity of clone 198, but not clone 252, was observed despite identical MPER epitope specificities and with usage of the same IgH and IgLk V genes by both rMAbs. Similar results demonstrating MPER/liposome reactivity independent of polyreactivity were obtained with a different pair of rMAbs, 219 and 196. These data suggest a critical role of the CDRH3s of both clones 252 and 219 in determining MPER specificity. Given that the MPER binding affinities of the rMAbs are also affected by interchanged pairings of IgH and IgLk, it appears that the fine specificity of anti-MPER rMAbs requires a structural fitness of the antibody combining site shaped by affinity maturation of B cells. In addition, and perhaps more importantly, the results demonstrate that not all MPER-specific antibodies are inherently polyspecific and/or autoreactive: polyreactivity of the MPER-specific rMAbs is separable from antigen specificity in these examples. Our findings are supported by a recent work characterizing a CD4-binding-site-specific BNAb lineage over time which tracked polyreactivity and antigen specificity and found that precursors were capable of obtaining and losing polyreactive characteristics independently of their progression toward the final BNAb (67). Whether the nonspecific liposome binding and polyreactivity independent of MPER specificity of 252M result from increased flexibility of CDRH3 and/or hydrophobicity introduced by sequence changes remains to be tested. In line with these results, increased polyspecificity was observed with alterations of the length and hydrophobic mutations of CDRH3 of 2F5 (29). Mispairings of IgH and IgL among 10E8 variants also increased polyreactivity (68).

The majority of the rMAbs specific for the MPER manifested weak or no liposome binding (DOPC/DOPG), with only several rMAbs showing qualitatively modest lipid binding, in-

cluding clone 219 (Fig. 4 and 9). In this regard, the recent crystal structure of 4E10 in complex with lipids showed a CDRH1 loop interaction with the lipid head groups and a CDRH3 loop interaction with the hydrophobic acyl chains, emphasizing that lipids appear to be an integral component of the 4E10 epitope (22). Given that the MPER immunogen is embedded in the lipid membrane, it would be interesting to test whether the MPER-specific rMAbs we generated recognize lipids differentially as part of their epitope and the extent to which the lipid interaction observed is linked structurally to polyspecificity as a by-product.

Elicitation of MPER-specific BNAbs has proven difficult. Given the polyreactivity and autoreactivity of 2F5 and 4E10, it has been suggested that immune tolerance mechanisms might limit the elicitation of broadly neutralizing HIV-1 antibodies (47, 50). This hypothesis was further supported by impaired B cell development in knock-in mice expressing the 2F5 or 4E10 V_HDJ_H and V_LJ_L rearrangements (69, 70). 2F5 V_H-V_L knock-in mice showed profound deletion of BNAb-expressing B cells in BM at the first tolerance checkpoint, when naive B cells begin to express surface BCR (70). A similar finding was observed for 4E10, for which various mechanisms of negative selection, including receptor editing, clonal deletion, and BCR downmodulation, were noted (69). Human kynureninase and splice factor 3B subunit 3 were identified, through a clever screening strategy, as conserved vertebrate self-antigens recognized by 2F5 and 4E10, respectively (47). Another screen, looking for 4E10 cross-reactivity and spanning a library from the human proteome, did not identify the splicing factor 3B subunit 3 autoreactivity candidate (71). Nonetheless, further support for the 2F5-kynureninase association comes from immunization of opossums, whose kynureninase orthologue lacks the ELDKWA epitope, instead containing the related but distinct ELEKWA sequence. These animals generate high antibody titers to the gp41 2F5 motif, in contrast to mice and other species (47).

While it appears that the aforementioned tolerance mechanisms may preclude or severely limit the generation of BNAbs against the MPER, an increasing number of naturally infected HIV patients produce MPER antibodies, including those with neutralizing activity (6, 72–75). Such antibodies develop without clinical evidence of autoimmune sequelae. Therefore, the difficulty in generating BNAbs directed at the MPER via immunization may relate primarily to issues of immunogenicity. In this respect, our earlier work (42) revealed how immunogenicity is dominated by residue accessibility. Sequence changes or modifications of MPER orientation relative to the membrane easily modulate immune responses and immunodominance. Whereas antibodies with specificity for a 2F5-like epitope were not elicited by the Npalm-MPER/liposome vaccine, 30 to 40% of MPER-specific plasma cells were directed to the N-terminal region of the MPER as assessed by ELISPOT assay when mice were immunized with mutant MPER Npalm-W680A/liposomes or MPERTM/liposomes, the latter of which contain the transmembrane region of gp41 (42; data not shown). Further characterization of rMAbs generated with the mutant MPER Npalm-W680A/liposome vaccine showed that the ELDKWA residues in the 2F5 epitope are critical for antibody binding, including a modest binding contribution from the K and A residues. The observation that MPER/liposome vaccines elicited strong humoral responses in BALB/c mice in our study but not in comparably immunized B6 mice (45) emphasizes how strain differences in inbred mice alter the outcome of the immune response. Our results also highlight that the context of immunogen presentation, including its precise three-dimensional display and sequence, plays a critical role in humoral responses by modulating B cell selection.

The present work reveals that MPER-specific antibodies recognizing a common epitope can be generated from genetically diverse germ line B cells without confinement to a specific gene usage but manifesting different functional characteristics. Some rMAbs exhibit polyspecificity, yet the majority do not share this feature. In keeping with our results, even though the 10E8 epitope overlaps that of 4E10, these MAbs manifest low and high polyreactivities/autoreactivities, respectively (51), and demonstrate different modes of binding (6, 21, 22). The discovery of 10E8 strongly implies that nonautoreactive BNAbs exist and can be elicited. Consistent with this notion, extensive screening of the rMAb 10E8 on an array of >9,400 human proteins showed modest cross-reactivity with only one protein, the intracellularly localized FAM84A protein (51).

We suggest that the polyclonality of B cells responding to the MPER peptide immunogen in a liposome context allows the immune system to generate a productive humoral response. While some of the theoretically possible responders in the repertoire may be removed before they emerge into the periphery due to mechanisms revealed through the B cell developmental studies of 4E10 and 2F5, others lacking polyreactivity/autoreactivity can progress to LLPC. Thus, the MPER target itself in a membrane context will not preclude the generation of protective antibodies. It is also notable that we demonstrate here an ability to derive LLPC comprising several percentage points of the total BM niche, with persistence of antibody production, over a very substantial fraction of the mouse lifetime. These antibodies recognize an epitope mapping to the 10E8 region, spanning the region from S668 to the end of the segment, but unlike 10E8, they are nonneutralizing. The lack of neutralization activity is due in part to the fact that they recognize the artificial C-terminal NH_2 group (42). Eliminating this C-terminal NH_2 group dependence while mimicking a more native structural configuration of the MPER likely will demand further modification of the MPER/liposome immunogen and may require inclusion of the transmembrane domain of gp41. Collectively, our data suggest that the greatest challenge to BNAb generation will be the design of vaccines to foster the correct immunogenicity targeting the native MPER exposed on the viral membrane-bound trimer.

ACKNOWLEDGMENTS

We thank Rachel Barry for her expert operation of the micromanipulator for single MPER-specific cell isolation, Hedda Wardemann for kindly providing the heavy and light chain vectors for recombinant antibody expression, and Peter Kwong for kindly providing the 10E8 antibody as well as a plasmid for expression of the 2F5 antibody.

This work was supported by funds from the Bill and Melinda Gates Foundation (grant OPP1108179) and the National Institute of Allergy and Infectious Diseases (NIAID) (grant U19 AI091693). S.M. and S.H.K. were supported in part by NIAID grant R01AI104739. D.I. is an investigator of the Howard Hughes Medical Institute.

FUNDING INFORMATION

This work, including the efforts of Luke R. Donius, Yuxing Cheng, Jaewon Choi, Zhen-Yu J. Sun, Melissa Hanson, Michael Zhang, Darrell Irvine, Ellis L. Reinherz, and Mikyung Kim, was funded by HHS | NIH | National Institute of Allergy and Infectious Diseases (NIAID) (AI091693). This work, including the efforts of Susanna Marquez, Mohammed Uduman, and Steven H. Kleinstein, was funded by HHS | NIH | National Institute of Allergy and Infectious Diseases (NIAID) (AI104739). This work, including the efforts of Melissa Hanson, Michael Zhang, and Darrell Irvine, was funded by Howard Hughes Medical Institute (HHMI). This work, including the efforts of Luke R. Donius, Yuxing Cheng, Jaewon Choi, Zhen-Yu J. Sun, Melissa Hanson, Michael Zhang, Darrell Irvine, Ellis L. Reinherz, and Mikyung Kim, was funded by Bill and Melinda Gates Foundation (Bill & Melinda Gates Foundation) (OPP1108179).

REFERENCES

1. **Plotkin SA.** 2013. Complex correlates of protection after vaccination. Clin Infect Dis **56:**1458–1465. http://dx.doi.org/10.1093/cid/cit048.
2. **Kwong PD, Mascola JR, Nabel GJ.** 2013. Broadly neutralizing antibodies and the search for an HIV-1 vaccine: the end of the beginning. Nat Rev Immunol **13:**693–701. http://dx.doi.org/10.1038/nri3516.
3. **Mascola JR, Haynes BF.** 2013. HIV-1 neutralizing antibodies: understanding nature's pathways. Immunol Rev **254:**225–244. http://dx.doi.org/10.1111/imr.12075.
4. **Halper-Stromberg A, Nussenzweig MC.** 2016. Towards HIV-1 remission: potential roles for broadly neutralizing antibodies. J Clin Invest **26:**415–423. http://dx.doi.org/10.1172/JCI80561.
5. **Buchacher A, Predl R, Strutzenberger K, Steinfellner W, Trkola A, Purtscher M, Gruber G, Tauer C, Steindl F, Jungbauer A.** 1994. Generation of human monoclonal antibodies against HIV-1 proteins; electrofusion and Epstein-Barr virus transformation for peripheral blood lymphocyte immortalization. AIDS Res Hum Retroviruses **10:**359–369. http://dx.doi.org/10.1089/aid.1994.10.359.
6. **Huang J, Ofek G, Laub L, Louder MK, Doria-Rose NA, Longo NS, Imamichi H, Bailer RT, Chakrabarti B, Sharma SK, Alam SM, Wang T, Yang Y, Zhang B, Migueles SA, Wyatt R, Haynes BF, Kwong PD, Mascola JR, Connors M.** 2012. Broad and potent neutralization of HIV-1 by a gp41-specific human antibody. Nature **491:**406–412. http://dx.doi.org/10.1038/nature11544.
7. **Ofek G, Zirkle B, Yang Y, Zhu Z, McKee K, Zhang B, Chuang GY, Georgiev IS, O'Dell S, Doria-Rose N, Mascola JR, Dimitrov DS, Kwong PD.** 2014. Structural basis for HIV-1 neutralization by 2F5-like antibodies m66 and m66.6. J Virol **88:**2426–2441. http://dx.doi.org/10.1128/JVI.02837-13.
8. **Morris L, Chen X, Alam M, Tomaras G, Zhang R, Marshall DJ, Chen B, Parks R, Foulger A, Jaeger F, Donathan M, Bilska M, Gray ES, Abdool Karim SS, Kepler TB, Whitesides J, Montefiori D, Moody MA, Liao HX, Haynes BF.** 2011. Isolation of a human anti-HIV gp41 membrane proximal region neutralizing antibody by antigen-specific single B cell sorting. PLoS One **6:**e23532. http://dx.doi.org/10.1371/journal.pone.0023532.
9. **Muster T, Steindl F, Purtscher M, Trkola A, Klima A, Himmler G, Rüker F, Katinger H.** 1993. A conserved neutralizing epitope on gp41 of human immunodeficiency virus type 1. J Virol **67:**6642–6647.
10. **Nelson JD, Brunel FM, Jensen R, Crooks ET, Cardoso RM, Wang M, Hessell A, Wilson IA, Binley JM, Dawson PE, Burton DR, Zwick MB.** 2007. An affinity-enhanced neutralizing antibody against the membrane-proximal external region of human immunodeficiency virus type 1 gp41 recognizes an epitope between those of 2F5 and 4E10. J Virol **81:**4033–4043. http://dx.doi.org/10.1128/JVI.02588-06.
11. **Zhu Z, Qin HR, Chen W, Zhao Q, Shen X, Schutte R, Wang Y, Ofek G, Streaker E, Prabakaran P, Fouda GG, Liao HX, Owens J, Louder M, Yang Y, Klaric KA, Moody MA, Mascola JR, Scott JK, Kwong PD, Montefiori D, Haynes BF, Tomaras GD, Dimitrov DS.** 2011. Cross-reactive HIV-1-neutralizing human monoclonal antibodies identified from a patient with 2F5-like antibodies. J Virol **85:**11401–11408. http://dx.doi.org/10.1128/JVI.05312-11.
12. **Zwick MB, Labrijn AF, Wang M, Spenlehauer C, Saphire EO, Binley JM, Moore JP, Stiegler G, Katinger H, Burton DR, Parren PW.** 2001. Broadly neutralizing antibodies targeted to the membrane-proximal external region of human immunodeficiency virus type 1 glycoprotein gp41. J Virol **75:**10892–10905. http://dx.doi.org/10.1128/JVI.75.22.10892-10905.2001.
13. **Burton DR, Mascola JR.** 2015. Antibody responses to envelope glycoproteins in HIV-1 infection. Nat Immunol **16:**571–576. http://dx.doi.org/10.1038/ni.3158.
14. **West AP, Scharf L, Scheid JF, Klein F, Bjorkman PJ, Nussenzweig MC.** 2014. Structural insights on the role of antibodies in HIV-1 vaccine and therapy. Cell **156:**633–648. http://dx.doi.org/10.1016/j.cell.2014.01.052.
15. **Salzwedel K, West JT, Hunter E.** 1999. A conserved tryptophan-rich motif in the membrane-proximal region of the human immunodeficiency virus type 1 gp41 ectodomain is important for Env-mediated fusion and virus infectivity. J Virol **73:**2469–2480.
16. **Sun Z-YJ, Cheng Y, Kim M, Song L, Choi J, Kudahl UJ, Brusic V, Chowdhury B, Yu L, Seaman MS, Bellot G, Shish WM, Wagner G, Reinherz EL.** 2014. Disruption of helix-capping residues 671 and 674 reveals a role in HIV-1 entry for a specialized hinge segment of the membrane proximal external region of gp41. J Mol Biol **426:**1095–1108. http://dx.doi.org/10.1016/j.jmb.2013.09.030.
17. **Montero M, van Houten NE, Wang X, Scott JK.** 2008. The membrane-proximal external region of the human immunodeficiency virus type 1 envelope: dominant site of antibody neutralization and target for vaccine design. Microbiol Mol Biol Rev **72:**54–84. http://dx.doi.org/10.1128/MMBR.00020-07.
18. **Sun ZY, Oh KJ, Kim M, Yu J, Brusic V, Song L, Qiao Z, Wang JH, Wagner G, Reinherz EL.** 2008. HIV-1 broadly neutralizing antibody extracts its epitope from a kinked gp41 ectodomain region on the viral membrane. Immunity **28:**52–63. http://dx.doi.org/10.1016/j.immuni.2007.11.018.
19. **Kim M, Sun ZY, Rand KD, Shi X, Song L, Cheng Y, Fahmy AF, Majumdar S, Ofek G, Yang Y, Kwong PD, Wang JH, Engen JR, Wagner G, Reinherz EL.** 2011. Antibody mechanics on a membrane-bound HIV segment essential for GP41-targeted viral neutralization. Nat Struct Mol Biol **18:**1235–1243. http://dx.doi.org/10.1038/nsmb.2154.
20. **Song L, Sun ZY, Coleman KE, Zwick MB, Gach JS, Wang JH, Reinherz EL, Wagner G, Kim M.** 2009. Broadly neutralizing anti-HIV-1 antibodies disrupt a hinge-related function of gp41 at the membrane interface. Proc Natl Acad Sci U S A **106:**9057–9062. http://dx.doi.org/10.1073/pnas.0901474106.
21. **Lee JH, Ozorowski G, Ward AB.** 2016. Cryo-EM structure of a native, fully glycosylated, cleaved HIV-1 envelope trimer. Science **351:**1043–1048. http://dx.doi.org/10.1126/science.aad2450.
22. **Irimia A, Sarkar A, Stanfield RL, Wilson IA.** 2016. Crystallographic identification of lipid as an integral component of the epitope of HIV broadly neutralizing antibody 4E10. Immunity **44:**21–31. http://dx.doi.org/10.1016/j.immuni.2015.12.001.
23. **Bellamy-McIntyre AK, Lay C-S, Baär S, Maerz AL, Talbo GH, Drummer HE, Poumbourios P.** 2007. Functional links between the fusion peptide-proximal polar segment and membrane-proximal region of human immunodeficiency virus gp41 in distinct phases of membrane fusion. J Biol Chem **282:**23104–23116. http://dx.doi.org/10.1074/jbc.M703485200.
24. **Muñoz-Barroso I, Salzwedel K, Hunter E, Blumenthal R.** 1999. Role of the membrane-proximal domain in the initial stages of human immunodeficiency virus type 1 envelope glycoprotein-mediated membrane fusion. J Virol **73:**6089–6092.
25. **Poumbourios P, Ahmar EW, McPhee DA, Kemp BE.** 1995. Determinants of human immunodeficiency virus type 1 envelope glycoprotein oligomeric structure. J Virol **69:**1209–1218.
26. **Alam SM, Morelli M, Dennison SM, Liao H-X, Zhang R, Xia S-M, Rits-Volloch S, Sun L, Harrison SC, Haynes BF, Chen B.** 2009. Role of HIV membrane in neutralization by two broadly neutralizing antibodies. Proc Natl Acad Sci U S A **106:**20234–20239. http://dx.doi.org/10.1073/pnas.0908713106.
27. **Sanchez-Martinez S, Lorizate M, Hermann K, Kunert R, Basanez G, Nieva JL.** 2006. Specific phospholipid recognition by human immunodeficiency virus type-1 neutralizing anti-gp41 2F5 antibody. FEBS Lett **580:**2395–2399. http://dx.doi.org/10.1016/j.febslet.2006.03.067.
28. **Ofek G, Guenaga FJ, Schief WR, Skinner J, Baker D, Wyatt R, Kwong PD.** 2010. Elicitation of structure-specific antibodies by epitope scaffolds. Proc Natl Acad Sci U S A **107:**17880–17887. http://dx.doi.org/10.1073/pnas.1004728107.
29. **Ofek G, McKee K, Yang Y, Yang ZY, Skinner J, Guenaga FJ, Wyatt R, Zwick MB, Nabel GJ, Mascola JR, Kwong PD.** 2010. Relationship between antibody 2F5 neutralization of HIV-1 and hydrophobicity of its

heavy chain third complementarity-determining region. J Virol **84:**2955–2962. http://dx.doi.org/10.1128/JVI.02257-09.
30. **Xu H, Song L, Kim M, Holmes MA, Kraft Z, Sellhorn G, Reinherz EL, Stamatatos L, Strong RK.** 2010. Interactions between lipids and human anti-HIV antibody 4E10 can be reduced without ablating neutralizing activity. J Virol **84:**1076–1088. http://dx.doi.org/10.1128/JVI.02113-09.
31. **Ofek G, Tang M, Sambor A, Katinger H, Mascola JR, Wyatt R, Kwong PD.** 2004. Structure and mechanistic analysis of the anti-human immunodeficiency virus type 1 antibody 2F5 in complex with its gp41 epitope. J Virol **78:**10724–10737. http://dx.doi.org/10.1128/JVI.78.19.10724-10737.2004.
32. **Cardoso RM, Zwick MB, Stanfield RL, Kunert R, Binley JM, Katinger H, Burton DR, Wilson IA.** 2005. Broadly neutralizing anti-HIV antibody 4E10 recognizes a helical conformation of a highly conserved fusion-associated motif in gp41. Immunity **22:**163–173. http://dx.doi.org/10.1016/j.immuni.2004.12.011.
33. **Scherer EM, Leaman DP, Zwick MB, McMichael AJ, Burton DR.** 2010. Aromatic residues at the edge of the antibody combining site facilitate viral glycoprotein recognition through membrane interactions. Proc Natl Acad Sci U S A **107:**1529–1534. http://dx.doi.org/10.1073/pnas.0909680107.
34. **Julien JP, Huarte N, Maeso R, Taneva SG, Cunningham A, Nieva JL, Pai EF.** 2010. Ablation of the complementarity-determining region H3 apex of the anti-HIV-1 broadly neutralizing antibody 2F5 abrogates neutralizing capacity without affecting core epitope binding. J Virol **84:**4136–4147. http://dx.doi.org/10.1128/JVI.02357-09.
35. **Zwick MB, Komori HK, Stanfield RL, Church S, Wang M, Parren PW, Kunert R, Katinger H, Wilson IA, Burton DR.** 2004. The long third complementarity-determining region of the heavy chain is important in the activity of the broadly neutralizing anti-human immunodeficiency virus type 1 antibody 2F5. J Virol **78:**3155–3161. http://dx.doi.org/10.1128/JVI.78.6.3155-3161.2004.
36. **Ingale S, Gach JS, Zwick MB, Dawson PE.** 2010. Synthesis and analysis of the membrane proximal external region epitopes of HIV-1. J Pept Sci **16:**716–722. http://dx.doi.org/10.1002/psc.1325.
37. **Cardoso RM, Brunel FM, Ferguson S, Zwick M, Burton DR, Dawson PE, Wilson IA.** 2007. Structural basis of enhanced binding of extended and helically constrained peptide epitopes of the broadly neutralizing HIV-1 antibody 4E10. J Mol Biol **365:**1533–1544. http://dx.doi.org/10.1016/j.jmb.2006.10.088.
38. **Correia BE, Ban YE, Holmes MA, Xu H, Ellingson K, Kraft Z, Carrico C, Boni E, Sather DN, Zenobia C, Burke KY, Bradley-Hewitt T, Bruhn-Johannsen JF, Kalyuzhniy O, Baker D, Strong RK, Stamatatos L, Schief WR.** 2010. Computational design of epitope-scaffolds allows induction of antibodies specific for a poorly immunogenic HIV vaccine epitope. Structure **18:**1116–1126. http://dx.doi.org/10.1016/j.str.2010.06.010.
39. **Kong L, Sattentau QJ.** 2012. Antigenicity and immunogenicity in HIV-1 antibody-based vaccine design. J AIDS Clin Res **S8:**3.
40. **Dennison SM, Sutherland LL, Jaeger FH, Anasti KM, Parks R, Stewart S, Bowman C, Xia S-M, Zhang R, Shen X, Scearce RM, Ofek G, Yang Y, Kwong PD, Santra S, Liao H-X, Tomaras G, Letvin NL, Chen B, Alam SM, Haynes BF.** 2011. Induction of antibodies in rhesus macaques that recognize a fusion-intermediate conformation of HIV-1 gp41. PLoS One **6:**e27824. http://dx.doi.org/10.1371/journal.pone.0027824.
41. **Hanson MC, Abraham W, Crespo MP, Chen SH, Liu H, Szeto GL, Kim M, Reinherz EL, Irvine DJ.** 2015. Liposomal vaccines incorporating molecular adjuvants and intrastructural T-cell help promote the immunogenicity of HIV membrane-proximal external region peptides. Vaccine **33:**861–868. http://dx.doi.org/10.1016/j.vaccine.2014.12.045.
42. **Kim M, Song L, Moon J, Sun Z-YJ, Bershteyn A, Hanson M, Cain D, Goka S, Kelsoe G, Wagner G, Irvine D, Reinherz EL.** 2013. Immunogenicity of membrane-bound HIV-1 gp41 MPER segments is dominated by residue accessibility and modulated by stereochemistry. J Biol Chem **288:**31888–31901. http://dx.doi.org/10.1074/jbc.M113.494609.
43. **Serrano S, Araujo A, Apellániz B, Bryson S, Carravilla P, de la Arada I, Huarte N, Rujas E, Pai EF, Arrondo JL, Domene C, Jiménez MA, Nieva JL.** 2014. Structure and immunogenicity of a peptide vaccine, including the complete HIV-1 gp41 2F5 epitope: implications for antibody recognition mechanism and immunogen design. J Biol Chem **289:**6565–6580. http://dx.doi.org/10.1074/jbc.M113.527747.
44. **Watson DS, Szoka FC.** 2009. Role of lipid structure in the humoral immune response in mice to covalent lipid-peptides from the membrane proximal region of HIV-1 gp41. Vaccine **27:**4672–4683. http://dx.doi.org/10.1016/j.vaccine.2009.05.059.
45. **Zhang J, Alam SM, Bouton-Verville H, Chen Y, Newman A, Stewart S, Jaeger FH, Montefiori DC, Dennison SM, Haynes BF, Verkoczy L.** 2014. Modulation of nonneutralizing HIV-1 gp41 responses by an MHC-restricted TH epitope overlapping those of membrane proximal external region broadly neutralizing antibodies. J Immunol **192:**1693–1706. http://dx.doi.org/10.4049/jimmunol.1302511.
46. **Verkoczy L, Kelsoe G, Haynes BF.** 2014. HIV-1 envelope gp41 broadly neutralizing antibodies: hurdles for vaccine development. PLoS Pathog **10:**e1004073. http://dx.doi.org/10.1371/journal.ppat.1004073.
47. **Yang G, Holl TM, Liu Y, Li Y, Lu X, Nicely NI, Kepler TB, Alam SM, Liao HX, Cain DW, Spicer L, VandeBerg JL, Haynes BF, Kelsoe G.** 2013. Identification of autoantigens recognized by the 2F5 and 4E10 broadly neutralizing HIV-1 antibodies. J Exp Med **210:**241–256. http://dx.doi.org/10.1084/jem.20121977.
48. **Liao H-X, Chen X, Munshaw S, Zhang R, Marshall DJ, Vandergrift N, Whitesides JF, Lu X, Yu J-S, Hwang K-K, Gao F, Markowitz M, Heath SL, Bar KJ, Goepfert PA, Montefiori DC, Shaw GC, Alam SM, Margolis DM, Denny TN, Boyd SD, Marshal E, Egholm M, Simen BB, Hanczaruk B, Fire AZ, Voss G, Kelsoe G, Tomaras GD, Moody MA, Kepler TB, Haynes BF.** 2011. Initial antibodies binding to HIV-1 gp41 in acutely infected subjects are polyreactive and highly mutated. J Exp Med **208:**2237–2249. http://dx.doi.org/10.1084/jem.20110363.
49. **Trama AM, Moody MA, Alam SM, Jaeger FH, Lockwood B, Parks R, Lloyd KE, Stolarchuk C, Scearce R, Foulger A, Marshall DJ, Whitesides JF, Jeffries TL, Jr, Wiehe K, Morris L, Lambson B, Soderberg K, Hwang KK, Tomaras GD, Vandergrift N, Jackson KJ, Roskin KM, Boyd SD, Kepler TB, Liao HX, Haynes BF.** 2014. HIV-1 envelope gp41 antibodies can originate from terminal ileum B cells that share cross-reactivity with commensal bacteria. Cell Host Microbe **16:**215–226. http://dx.doi.org/10.1016/j.chom.2014.07.003.
50. **Haynes BF, Fleming J, St Clair EW, Katinger H, Stiegler G, Kunert R, Robinson J, Scearce RM, Plonk K, Staats HF, Ortel TL, Liao HX, Alam SM.** 2005. Cardiolipin polyspecific autoreactivity in two broadly neutralizing HIV-1 antibodies. Science **308:**1906–1908. http://dx.doi.org/10.1126/science.1111781.
51. **Liu M, Yang G, Wiehe K, Nicely NI, Vandergrift NA, Rountree W, Bonsignori M, Alam SM, Gao J, Haynes BF, Kelsoe G.** 2015. Polyreactivity and autoreactivity among HIV-1 antibodies. J Virol **89:**784–798. http://dx.doi.org/10.1128/JVI.02378-14.
52. **Ogunniyi AO, Story CM, Papa E, Guillen E, Love JC.** 2009. Screening individual hybridomas by microengraving to discover monoclonal antibodies. Nat Protoc **4:**767–782. http://dx.doi.org/10.1038/nprot.2009.40.
53. **Tiller T, Busse CE, Wardemann H.** 2009. Cloning and expression of murine Ig genes from single B cells. J Immunol Methods **350:**183–193. http://dx.doi.org/10.1016/j.jim.2009.08.009.
54. **Gupta NT, Vander Heiden JA, Uduman M, Gadala-Maria D, Yaari G, Kleinstein SH.** 2015. Change-O: a toolkit for analyzing large-scale B cell immunoglobulin repertoire sequencing data. Bioinformatics **31:**3356–3358. http://dx.doi.org/10.1093/bioinformatics/btv359.
55. **Yaari G, Uduman M, Kleinstein SH.** 2012. Quantifying selection in high-throughput immunoglobulin sequencing data sets. Nucleic Acids Res **40:**e134. http://dx.doi.org/10.1093/nar/gks457.
56. **Halliley JL, Tipton CM, Liesveld J, Rosenberg AF, Darce J, Gregoretti IV, Popova L, Kaminiski D, Fucile CF, Albizua I, Kyu S, Chiang KY, Bradley KT, Burack R, Slifka M, Hammarlund E, Wu H, Zhao L, Walsh EE, Falsey AR, Randall TD, Cheung WC, Sanz I, Lee FE.** 2015. Long-lived plasma cells are contained within the CD19(−)CD38(hi)CD138(+) subset in human bone marrow. Immunity **43:**132–145. http://dx.doi.org/10.1016/j.immuni.2015.06.016.
57. **Slifka MK, Antia R, Whitmire JK, Ahmed R.** 1998. Humoral immunity due to long-lived plasma cells. Immunity **8:**363–372. http://dx.doi.org/10.1016/S1074-7613(00)80541-5.
58. **Lazarski CA, Chaves FA, Jenks SA, Wu S, Richards KA, Weaver JM, Sant AJ.** 2005. The kinetic stability of MHC class II:peptide complexes is a key parameter that dictates immunodominance. Immunity **23:**29–40. http://dx.doi.org/10.1016/j.immuni.2005.05.009.
59. **Love JC, Ronan JL, Grotenbreg GM, van der Veen AG, Ploegh HL.** 2006. A microengraving method for rapid selection of single cells producing antigen-specific antibodies. Nat Biotechnol **24:**703–707. http://dx.doi.org/10.1038/nbt1210.
60. **Ogunniyi AO, Thomas BA, Politano TJ, Varadarajan N, Landais E, Poignard P, Walker BD, Kwon DS, Love JC.** 2014. Profiling human

antibody responses by integrated single-cell analysis. Vaccine **32:**2866–2873. http://dx.doi.org/10.1016/j.vaccine.2014.02.020.

61. **Yu L, Guan Y.** 2014. Immunologic basis for long HCDR3s in broadly neutralizing antibodies against HIV-1. Front Immunol **5:**250. http://dx.doi.org/10.3389/fimmu.2014.00250.
62. **Scheid JF, Mouquet H, Ueberheide B, Diskin R, Klein F, Oliveira TY, Pietzsch J, Fenyo D, Abadir A, Velinzon K, Hurley A, Myung S, Boulad F, Poignard P, Burton DR, Pereyra F, Ho DD, Walker BD, Seaman MS, Bjorkman PJ, Chait BT, Nussenzweig MC.** 2011. Sequence and structural convergence of broad and potent HIV antibodies that mimic CD4 binding. Science **333:**1633–1637. http://dx.doi.org/10.1126/science.1207227.
63. **West AP, Diskin R, Nussenzweig MC, Bjorkman PJ.** 2012. Structural basis for germ-line gene usage of a potent class of antibodies targeting the CD4-binding site of HIV-1 gp120. Proc Natl Acad Sci U S A **109:**E2083–E2090. http://dx.doi.org/10.1073/pnas.1208984109.
64. **Zhou T, Zhu J, Wu X, Moquin S, Zhang B, Acharya P, Georgiev IS, Altae-Tran HR, Chuang GY, Joyce MG, Do Kwon Y, Longo NS, Louder MK, Luongo T, McKee K, Schramm CA, Skinner J, Yang Y, Yang Z, Zhang Z, Zheng A, Bonsignor IM, Haynes BF, Scheid JF, Nussenzweig MC, Simek M, Burton DR, Koff WC, NISC Comparative Sequencing Program, Mullikin JC, Connors M, Shapiro L, Nabel GJ, Mascola JR, Kwong PD.** 2013. Multidonor analysis reveals structural elements, genetic determinants, and maturation pathway for HIV-1 neutralization by VRC01-class antibodies. Immunity **39:**245–258. http://dx.doi.org/10.1016/j.immuni.2013.04.012.
65. **Wu X, Yang ZY, Li Y, Hogerkorp CM, Schief WR, Seaman MS, Zhou T, Schmidt SD, Wu L, Xu L, Longo NS, McKee K, O'Dell S, Louder MK, Wycuff DL, Feng Y, Nason M, Doria-Rose N, Connors M, Kwong PD, Roederer M, Wyatt RT, Nabel GJ, Mascola JR.** 2010. Rational design of envelope identifies broadly neutralizing human monoclonal antibodies to HIV-1. Science **329:**856–861. http://dx.doi.org/10.1126/science.1187659.
66. **Ichiyoshi Y, Casali P.** 1994. Analysis of the structural correlates for antibody polyreactivity by multiple reassortments of chimeric human immunoglobulin heavy and light chain V segments. J Exp Med **180:**885–895. http://dx.doi.org/10.1084/jem.180.3.885.
67. **Bonsignori M, Zhou T, Sheng Z, Chen L, Gao F, Joyce MG, Ozorowski G, Chuang GY, Schramm CA, Wiehe K, Alam SM, Bradley T, Gladden MA, Hwang KK, Iyengar S, Kumar A, Lu X, Luo K, Mangiapani MC, Parks RJ, Song H, Acharya P, Bailer RT, Cao A, Druz A, Georgiev IS, Kwon YD, Louder MK, Zhang B, Zheng A, Hill BJ, Kong R, Soto C, NISC Comparative Sequencing Program, Mullikin JC, Douek DC, Montefiori DC, Moody MA, Shaw GM, Hahn BH, Kelsoe G, Hraber PT, Korber BT, Boyd SD, Fire AZ, Kepler TB, Shapiro L, Ward AB, Mascola JR, Liao HX, Kwong PD, Haynes BF.** 2016. Maturation pathway from germline to broad HIV-1 neutralizer of a CD4-mimic antibody. Cell **165:**449–463. http://dx.doi.org/10.1016/j.cell.2016.02.022.
68. **Zhu J, Ofek G, Yang Y, Zhang B, Louder MK, Lu G, McKee K, Pancera M, Skinner J, Zhang Z, Parks R, Eudailey J, Lloyd KE, Blinn J, Alam SM, Haynes BF, Simek M, Burton DR, Koff WC, NISC Comparative Sequencing Program, Mullikin JC, Mascola JR, Shapiro L, Kwong PD.** 2013. Mining the antibodyome for HIV-1-neutralizing antibodies with next-generation sequencing and phylogenetic pairing of heavy/light chains. Proc Natl Acad Sci U S A **110:**6470–6475. http://dx.doi.org/10.1073/pnas.1219320110.
69. **Doyle-Cooper C, Hudson KE, Cooper AB, Ota T, Skog P, Dawson PE, Zwick MB, Schief WR, Burton DR, Nemazee D.** 2013. Immune tolerance negatively regulates B cells in knock-in mice expressing broadly neutralizing HIV antibody 4E10. J Immunol **191:**3186–3191. http://dx.doi.org/10.4049/jimmunol.1301285.
70. **Verkoczy L, Chen Y, Bouton-Verville H, Zhang J, Diaz M, Hutchinson J, Ouyang YB, Alam SM, Holl TM, Hwang KK, Kelsoe G, Haynes BF.** 2011. Rescue of HIV-1 broad neutralizing antibody-expressing B cells in 2F5 VH × VL knockin mice reveals multiple tolerance controls. J Immunol **187:**3785–3797. http://dx.doi.org/10.4049/jimmunol.1101633.
71. **Finton KA, Larimore K, Larman HB, Friend D, Correnti C, Rupert PB, Elledge SJ, Greenberg PD, Strong RK.** 2013. Autoreactivity and exceptional CDR plasticity (but not unusual polyspecificity) hinder elicitation of the anti-HIV antibody 4E10. PLoS Pathog **9:**e1003639. http://dx.doi.org/10.1371/journal.ppat.1003639.
72. **Gray ES, Madiga MC, Moore PL, Mlisana K, Abdool Karim SS, Binley JM, Shaw GM, Mascola JR, Morris L.** 2009. Broad neutralization of human immunodeficiency virus type 1 mediated by plasma antibodies against the gp41 membrane proximal external region. J Virol **83:**11265–11274. http://dx.doi.org/10.1128/JVI.01359-09.
73. **Jacob RA, Moyo T, Schomaker M, Abrahams F, Pujol BG, Dorfman JR.** 2015. Anti-V3/glycan and anti-MPER neutralizing antibodies, but not anti-V2/glycan site antibodies, are strongly associated with greater anti-HIV-1 neutralization breadth and potency. J Virol **89:**5264–5275. http://dx.doi.org/10.1128/JVI.00129-15.
74. **Li Y, Svehla K, Louder MK, Wycuff D, Phogat S, Tang M, Migueles SA, Wu X, Phogat A, Shaw GM, Connors M, Hoxie J, Mascola JR, Wyatt R.** 2009. Analysis of neutralization specificities in polyclonal sera derived from human immunodeficiency virus type 1-infected individuals. J Virol **83:**1045–1059. http://dx.doi.org/10.1128/JVI.01992-08.
75. **Molinos-Albert LM, Carrillo J, Curriu M, Rodriguez de la Concepción ML, Marfil S, García E, Clotet B, Blanco J.** 2014. Anti-MPER antibodies with heterogeneous neutralization capacity are detectable in most untreated HIV-1 infected individuals. Retrovirology **11:**44. http://dx.doi.org/10.1186/1742-4690-11-44.
76. **Di Niro R, Lee S-J, Vander Heiden JA, Elsner RA, Trivedi N, Bannock JM, Gupta NT, Kleinstein SH, Vigneault F, Gilbert TJ, Meffre E, McSorley SJ, Shlomchik MJ.** 2015. Salmonella infection drives promiscuous B cell activation followed by extrafollicular affinity maturation. Immunity **43:**120–131. http://dx.doi.org/10.1016/j.immuni.2015.06.013.